Towards Flash Flood Modeling Using Gradient Resolving Representative Hillslopes

Ashish Manoj J[a,1], Ralf Loritz[1], Franziska Villinger[1], Mirko Mälicke[1], Mehdi Koopaeidar[1], Hans Göppert[2], Erwin Zehe[1]

[1] Institute of Water and River Basin Management – Hydrology, Karlsruhe Institute of Technology, Kaiserstrasse 12, 76131 Karlsruhe, Germany

[2] Wald + Corbe Consulting GmbH, Am Hecklehamm 18, 76549 Hügelsheim, Germany

[a] *Correspondence to*: Ashish Manoj J (ashish.jaseetha@kit.edu)

Ashish Manoj J (ashish.jaseetha@kit.edu)

Ralf Loritz (ralf.loritz@kit.edu)

Franziska Villinger (franziska.villinger@kit.edu)

Mirko Mälicke (mirko.maelicke@kit.edu)

Mehdi Koopaeidar (mehdi.ko11@gmail.com)

Hans Göppert (h.goeppert@wald-corbe.de)

Erwin Zehe (erwin.zehe@kit.edu)

Key Points

- Physically based representative hillslope models resolve the main gradients controlling overland flow, a key requirement for modelling flash floods in small, data-scarce and rural catchments.
- Climate reanalysis data enable the initialization of a process-based model, establishing plausible initial conditions for event-based flash flood modelling that can guide the design of retention basins in small to medium sized catchments.
- Transfer of model parameters from past experiments to data-scarce catchments within the same hydrological landscape is feasible and water level measurements at flood defense reservoir can be used for model building and testing.

Abstract

It is increasingly acknowledged that the acceleration of the global water cycle, largely driven by anthropogenic climate change, has a disproportionate impact on sub-daily and small-scale hydrological extreme events such as flash floods. These events occur thereby at local scales within minutes to hours, typically in response to high-intensity rainfall events associated with convective storms. Despite their local scale and rapid onset, the effects of flash floods can be devastating, making their prediction and mitigation of critical importance. However, the modeling and analysis of such events in data-scarce regions present a unique set of challenges. In the present work, we show that by employing physically based representative hillslope models that resolve the main gradients controlling overland flow hydrology and hydraulics, we can get reliable simulations of flash flood response in small data-scarce catchments. To this end, we use climate reanalysis products and transfer soil parameters previously obtained for hydrological predictions in an experimental catchment in the same landscape. The inverted mass balance of flood reservoirs downstream is employed to derive a target data set for model evaluation in these nearly ungauged basins. We show that our approach using representative hillslopes and climate datasets can provide reasonable uncalibrated estimates of the overland runoff response (flood magnitude, storm volume, and event runoff coefficients) in three of the four catchments considered. Given that flash floods typically occur at scales of a few km^2 and in ungauged places, our results have implications for operational flash flood forecasting and the design of small and medium flood retention basins around the world.

Plain Language Summary

Flash floods have become increasingly common worldwide, with catastrophic damages to both human life and the economy. While the extent of global warming and climate change impacting these events is still under much debate, it is almost certain now that we need to be better equipped to understand and model these extremes to prevent and mitigate the possible risk to human life and infrastructure in a warming climate. To test, if we can use first principles derived from thermodynamic conservation laws and process based hydrological models for the same, we modelled flash flood response in four headwater catchments over Southern Germany using the concept of 'representative hillslope'. Since the regions considered in our work are nearly ungauged, we made use of global climate reanalysis products and parameter transfer from past experiments. The encouraging results obtained in predicting the flood magnitude and volume speak to the overall applicability of our approach. We are able to get decent uncalibrated predictions in three out of the four catchments considered with minimum computational effort. However, as the results in one of the catchments show, further research and modelling experiments are required to advance the applied methodology for the design of flood mitigation measures and operational flash flood forecasting. Understanding and managing the adverse impacts of such extreme hydroclimatic events remains one of the crucial hurdles facing humanity towards the sustainable development goals (SDG17) in this decade.

Keywords – flash floods, ungauged basins, physically based models, parameter transfer, representative hillslopes.

1 Introduction

As early as 2008, the Organisation for Economic Co-operation and Development (OECD) highlighted climate change and hydro-meteorological extremes as some of the most pressing challenges facing humanity. Flood events, a key component of these extremes, manifest at varying spatial and temporal scales, each driven by distinct meteorological conditions. Flash floods, for instance, occur on local scales within a span of minutes to hours. These events are triggered by high-intensity rainfall from convective storms, resulting in infiltration excess and significant overland flow (Bronstert et al., 2018; Marchi et al., 2016, 2010; Meyer et al., 2022; Ruiz-Villanueva et al., 2012). While these floods pose immediate risks, such as loss of human life, their consequences extend to long-term impacts like soil erosion, sediment transport, and subsequent deterioration of water quality and soil fertility, particularly in agricultural settings. On the other end of the spectrum are large-scale riverine floods, which occur due to synoptic scale low-pressure systems characterized by widespread and sustained precipitation. Unlike flash floods, these events are governed by capacity-controlled runoff formation processes like saturation excess, known as Dunne overland flow (Dunne and Kirkby, 1978), and subsurface storm flow. Additionally, flood routing in channel networks and snowmelt contributions, play crucial roles (Blöschl et al., 2007). This stands in contrast to the Hortonian overland flow (Horton, 1933) typically observed in flash floods driven by convective storms.

Flood forecasting and risk management have to cope with both types of flood events, and both are naturally highly sensitive to climate change (IPCC, 2021). The largest observed floods in many European rivers have occurred in the last three decades, which count among the most flood-rich periods in the past 500 years (Blöschl et al., 2020). With respect to local flash floods, the situation seems not better. For instance, 22 flash floods in southwest Germany occurring in the past 20 years, had estimated design return periods exceeding 500 years (Göppert, 2018). This is in line with the recent accumulation of flash floods in Europe (Meyer et al., 2022), which likely reflects the already ongoing acceleration of the hydrological cycle, with expected increasing frequencies of more intense convective rainstorms and flash floods due to Clausius-Clapeyron scaling (Pall et al., 2007). This is alarming, as the flash flood series in the summer of 2016 alone caused about €2.5 bn of damage in Germany (Munich Re, 2016). All this recent evidence calls for

115 improving the current standards in a) flood predictions and b) methods for deriving
116 hydrological extreme values for design.

117 Considerable progress has been made in alert systems for riverine floods (Borga et al.,
118 2011; Thielen et al., 2009). These systems rely on ensemble numerical weather
119 predictions and conceptual hydrological models such as LARSIM (Bremicker, 1998), HBV
120 (Hundecha and Bardossy, 2004) or LISFLOOD (van der Knijff et al., 2010). Conceptual
121 hydrological models simulate rainfall-runoff generation using linear reservoir concepts
122 characterised by effective fluxes, states, and effective parameters (Hrachowitz and Clark,
123 2017). Despite their simplicity, countless studies have shown that they capture capacity-
124 controlled runoff generation processes quite well (Berkowitz and Zehe, 2020). Today it
125 is known that conceptual models provide reliable predictions of streamflow for
126 catchments larger than 200 km^2 (Zehe et al., 2014), explaining their widespread and
127 successful operational use.

128 Despite their success, conceptual models, like every model, also have limitations. They
129 usually give lumped integral responses and do not provide detailed information on how
130 each principal component within the model interacts (Fatichi et al., 2016). Predictions
131 are also subject to model structural uncertainty as several parameter sets may reproduce
132 the target discharge data within the learning phase in an acceptable manner (Beven and
133 Binley, 1992). While multi-response calibration is generally well suited to reduce
134 parameter uncertainty, this venture is not straightforward in the case of conceptual
135 models, as their parameters and states cannot be measured directly (Berkowitz and Zehe,
136 2020; Hrachowitz and Clark, 2017). This has crucial implications for the transfer of such
137 models to ungauged regions. In most cases, they do not perform well in regions outside
138 their calibrated range. In the context of flash flooding this is of key importance, as these
139 events are rare, typically impacting small catchments or even specific hillslopes which
140 are often ungauged. They are thus tricky and challenging to observe with conventional
141 rain and discharge measurement networks (Borga et al., 2008), which implies that the
142 sample for model learning and testing is small. Hence they are strongly related to the
143 classical 'predictions in ungauged basins - PUB problem' (Hrachowitz et al., 2013;
144 Sivapalan et al., 2003), which implies the estimation of either the occurrence frequency
145 or forecasting the hydrological response using current/future climate and topographic
146 inputs without the benefit of past observational time series for direct model calibration.

Here, we propose that gradient resolving, physically based hydrological models (Fatichi et al., 2016; Paniconi and Putti, 2015) are well suited to address the challenges of flash flood predictions in such data scarce regions. By solving coupled partial differential equations (PDEs) that represent infiltration, soil moisture dynamics, runoff, streamflow and evaporation in space and time, such models allow for spatially distributed simulations of extreme flash floods (Pérez et al., 2011; Steinbrich et al., 2016; Zehe et al., 2001).

Our primary aim is to evaluate the efficacy of gradient-resolving, physically based hydrological models for predicting flash floods triggered by convective rainstorms in data-scarce regions. Further, we aim to explore the feasibility of operationalizing these models for the design of small and medium reservoirs in such regions. One of the primary challenges in employing physically based models lies in their 'data greed,' requiring extensive input data, as well as the computational expense involved in running the models. To mitigate the data requirement challenge, we propose to leverage existing information from well-studied past catchments within the same hydrological landscape. Specifically, we suggest utilizing these well-instrumented catchments as 'donor catchments' to transfer model structures and parameters to target catchments that are poorly instrumented but share similar hydrological characteristics (Figures 1 & 2T). Specifically, we explore:

1. Is it feasible to transfer model parameters from a past monitored experimental catchment to data-scarce catchments for uncalibrated flash flood predictions in response to increased convective storm activity?
2. To overcome the computational expense challenge, we explore whether *the representative hillslope* concept (Loritz. et al. 2017; see section 3.1) is an effective way to reduce computation burden, while maintaining a balance between model complexity and data requirements?

As study areas, we selected several headwaters upstream of flood defence reservoirs in South West Germany, operated by the Elsenz-Schwarzbach Water Board (Zweckverband Hochwasserschutz Elsenz-Schwarzbach, 2016). In June 2016, several of these flood reservoirs were overtopped in response to a convective rainstorm. While these catchments are in the same hydrological landscape as the previously monitored Weiherbach experimental headwater shed (Zehe et al., 2001), they are, despite the

available water level gauges in the reservoirs, completely unmonitored with respect to rainfall, streamflow and soil moisture. To overcome the related challenges, we investigate:

3. Can climate reanalysis data initialize process-based hydrological models and transition to higher-resolution radar precipitation data without requiring recalibration during flood simulations?
4. Is reservoir mass balance inversion a reliable method for estimating storm hydrographs during flash flood events and how does the inherent uncertainty of such floods affect design considerations?

2 Venue and Model

2.1 Study Area

The four headwater catchments (in this study referred to as W22, W32, W39 and W44) belong to the Elsenz-Schwarzbach catchment in the State of Baden Württemberg, Southern Germany (Figure 1 & Figure B1 in Appendix B). The catchment is located within the eastern "Kraichgau", west of Bad Rappenau and around 50 km from the nearest cities - Heidelberg and Karlsruhe. Due to a series of catastrophic flooding episodes in 1993-94, a comprehensive flood protection concept for the entire region was envisaged, which led to the development of local flood retention basins throughout the catchment area. The size of the catchments varies from 1-6 km^2; they all drain into the Krebsbach, which joins into the Schwarzbach near Waibstadt (the nearest gauging station – Eschelbronn Schwarzbach, being more than 12km from our study area). The Elsenz-Schwarzbach finally merges into the Neckar, one of the Rhine's largest tributaries. From Figure 1, it is clear that even though the catchments are primarily agricultural in nature (major crops being – cereals, maize, sugar beets and potatoes), they are situated upstream of the population centres of the region. As flooding could have catastrophic impacts on human life and establishment, these settlements have been protected by regulated flood defence reservoirs.

During the end of May to early June 2016, several strong convective rainfall events clustered in Germany because of persistent atmospheric conditions (Bronstert et al., 2018; Meyer et al., 2022; Piper et al., 2016). Rain totals exceeding 100 mm were reported in a day, triggering flash floods in many small catchments over Southern Germany. The impacts in the Elsenz-Schwarzbach were also severe, with several of the flood control

reservoirs being overtopped. To investigate the feasibility of our approach (Figure 2) and of the CAFLOW model to simulate such events, we focus our attention on the severe event of 08 June 2016 in the region (Appendix -B). Since no streamflow gauges are available for the four headwater catchments, we use the water level measurements in the flood control reservoirs to estimate the runoff response based on the reconstructed reservoir inflow (W22, W32, W39 and W44). The storm runoff response is calculated based on inverting the reservoir mass balance with the knowledge of the reservoir geometry and stage-outflow relationship (Appendix-C). Related uncertainties are accounted for by using a relative percentage error value (5%) in the stage level measurements.

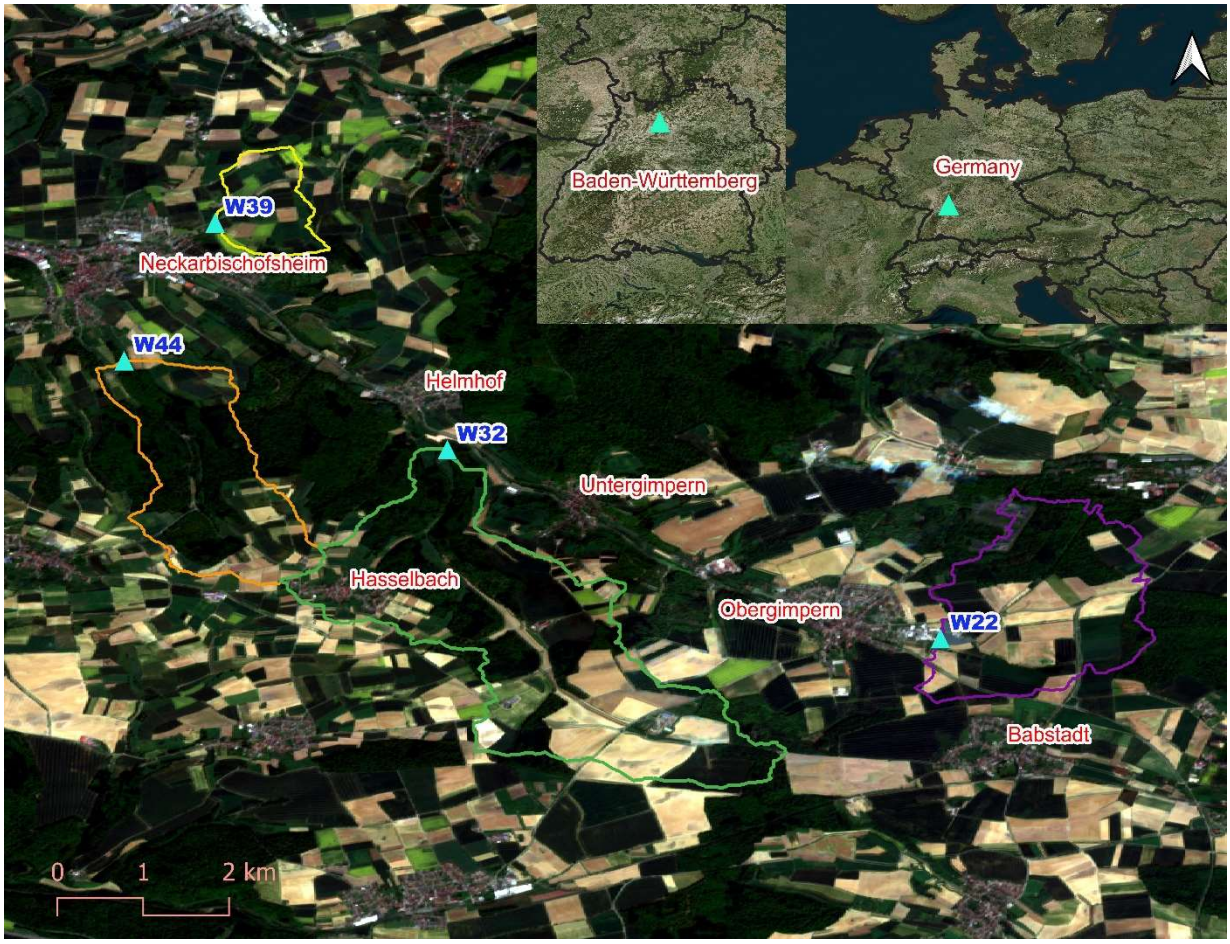

Figure 1 Overview of the location of the four headwater catchments considered in the study. Also, shown in the figure are the downstream flood control reservoirs, which afford protection to the towns in the region. The overlay layer depicts a Sentinel-2 (Drusch et al., 2012) multispectral true colour composite image showing the major land use patterns during May-June 2016. Figure B1 in Appendix B shows the stream network of Krebsbach and Schwarzbach and also the total accumulated precipitation during the event.

2.2 CATFLOW in a Nutshell

The quest for accurately identifying and modelling the governing processes of water balance and reactive pesticide transport in rural catchments motivated both the setup of the Weiherbach experimental catchment in the 90's (Plate and Zehe, 2008; Zehe et al., 2001) and the development of the process-based model CATFLOW (Zehe et al., 2001). The model relies on the subdivision of a catchment into several 2D hillslopes and an interconnected drainage (optional) and river network. However, each hillslope is modeled separately and hence this provides the opportunity to run each hillslope individually without the associated stream network. Hillslopes are discretised along a two- dimensional cross section using terrain following curvilinear orthogonal coordinates. Soil water dynamics within the hillslopes are characterized using the potential based form of the 2D Darcy–Richards equation, solved by a mass conservative Picard solver using adaptive time stepping (Celia and Bouloutas, 1990). Soil hydraulic properties can be parameterised according to van Genuchten (1980) and Mualem (1976), Tang and Skaggs (1977) or the recently proposed PDI model (Peters et al., 2021)

Overland flow is simulated using the diffusion wave approximation of the Saint-Venant equation and explicit upstreaming, in combination with the Gauckler-Manning-Strickler formula. The model can optionally account for rills (Schroers et al., 2022), sediment transport (Schroers et al., 2023) and reactive transport of solutes (Klaus and Zehe, 2010). Evaporation and transpiration are usually simulated using a SVAT (Surface Vegetation – Atmosphere Transfer) module based on the Penman–Monteith equation, accounting for annual cycles of plant phenology, albedo, and roughness using tabulated data. Stomatal conductance is characterized after Jarvis (1976), or via the inversion of sap flow data (Loritz et al., 2022). CATFLOW has been used in numerous landscapes to explore watershed functioning, the predictability of (flash) flooding (Villinger et al., 2022; Zehe et al., 2005; Zehe and Blöschl, 2004) the role of subsurface storm flow for runoff generation (Loritz et al., 2017; Wienhofer and Zehe, 2014) or the value of distributed precipitation for improving stream flow predictions (Loritz et al., 2021; Zehe et al., 2005).

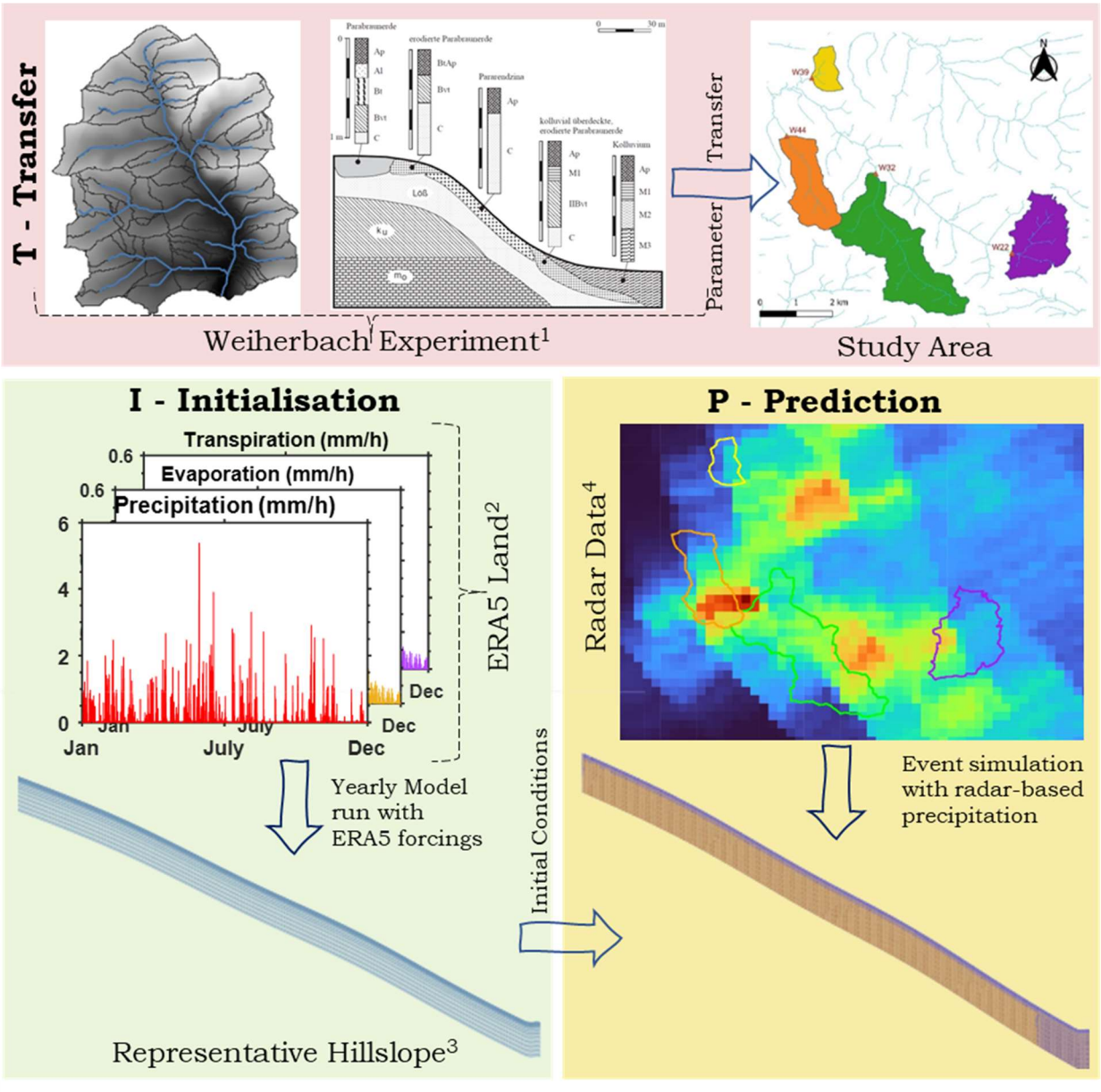

254 Figure 2 Illustration of our methodological approach– Transfer (T), Initialisation (I) and
255 Prediction (P). In Transfer (T), we transfer our knowledge of hillslope properties and soil
256 parameters from the Weiherbach to our study area in Krebsbach. The Initialisation (I) phase
257 involves deriving the representative hillslope (detailed in Figure 3) for the catchments and using
258 the ERA5 Land forcings to run the hillslope model for an entire year. In the prediction phase, (P),
259 the same model is run with the fine-resolution radar forcing and initial conditions from
260 Initialisation (I) for predicting the flash flood discharge. (1 -Zehe et al. (2001), 2 - Muñoz-Sabater
261 et al., (2021), 3 – Figure 3 & Loritz et al. (2017), 4 –Kachelmannwetter, n.d (Radar Data.)

3 Methodology

Setting up a process based model of any hydrological system mainly requires two types of information (Remson et al., 1971). The first one concerns the fundamental laws governing the dynamics of system state variables and fluxes and related process parametrizations (e.g., preferential macropore flow) related to the chosen model. The second involves the data representing the "landscape" in the equation set. A proper identification of these properties is crucial for reliable model performance, and they can be divided into a) system geometry, b) system parameters and c) initial and boundary (forcing) conditions. The current section details the steps required for setting up the model in this respect. We firstly explain the concept of the representative hillslope and its derivation from digital topographical data, then elaborate on the transfer of soil and land use parameters from the Weiherbach. Finally, we explain the spin up of the model using ERA5 Land and the radar-based precipitation product used during the event simulation.

3.1 The representative hillslope concept

Physically based hydrological models are renowned for their substantial computational demands, often impeding their broader application (Paniconi and Putti, 2015). As a result, catchment hydrology research has pivoted towards simplifying these models, ensuring they retain their physical underpinnings. Notable models that exemplify this approach include the hillslope storage Boussinesq model by Troch et al. (2003) and the representative elementary watershed model proposed by Reggiani et al. (1998). In this study, we adopt a gradient-based simplification termed 'representative hillslopes', as introduced by Loritz et al. (2017). Their work demonstrated that the water balance and streamflow generation in the Colpach catchment (19 km^2) could be accurately simulated using a single representative hillslope, negating the need for an associated river network.

Here we provide a concise explanation on why this approach works. The concept behind a *representative hillslope* is that both surface and subsurface water fluxes are propelled by differences in potential energy (Loritz et al., 2017; Zehe et al., 2013). These differences emerge from rainfall distribution over varied topography. In the context of intense convective rainstorms, our focus narrows to the energy balance of overland flow. Here, the driving potential energy difference hinges on the relative elevation between a location and its corresponding flow outlet. It's crucial to recognize that only a minute portion of this potential energy is converted into overland flow kinetic energy, with the

majority being dissipated, primarily influenced by factors such as Manning's roughness (Schroers et al., 2022).

Preserving this energy dynamic implies that the topography of the representative hillslope should be structured to maintain average topographic gradients along the flow path to the nearest drainage point. A viable method involves segmenting geo-potential energy by proximity to the river and averaging within each segment. Specifically, we consider the distribution of flow profile lines shown in Figure 3B for catchment W22. For any distance class (also shown in Figure A1: Appendix – A), the total flow potential is the sum of all the potential of the cells within the class, which is proportional to the relative elevation difference of the cells. For the catena profile, we require a representative value for this class so that the total energy remains conserved. We use the Linear Average Representative Slope Profile concept from Francke et al. (2008) for the same. The method involves a weighting factor based on the relative occurrence of each cell in a flow path (characterised by the flow accumulation values). Therefore, the value of the mean elevation (h_i) for a class at distance i:

$$h_i = \frac{\sum_{j=1}^{n} h_j \sqrt{f_j}}{\sum_{j=1}^{n} \sqrt{f_j}} \qquad (3.1)$$

where h_j & f_j are the relative elevation and flow accumulation values for each cell in the class at a distance i and $j: 1\ to\ n$ be the total number of cells in the class. The representative value for any other attribute (say width) can also be calculated similarly.

3.2 System Geometry (Deriving the hillslope profile)

The representative hillslope topography is derived for each of the four catchments (Fig 1) as illustrated for the catchment W22 in Fig 3. Firstly, the digital elevation model (DEM) is pre-processed to fill all depressions and sinks. We then derive the flow accumulation, aspect, and stream rasters from this filled DEM. The distance to the river and elevation to river rasters (which indicates the relative horizontal and vertical distance from a cell to the nearest river segment, respectively) are then extracted.

The distance from the nearest river segment and the corresponding relative elevation difference is plotted for all the cells within the catchment of interest (Fig 3B). In Fig 3B, each green dot denotes a 10 x 10 m^2 cell in the catchment. The representative hillslope catena is then derived based on the methodology explained in Section 3.1. The potential energy conservation along the direction of the flow profile by means of the weighted

mean elevation values is validated using four different distance classes (100m, 200m, 300m & 400m: Fig A1) in Appendix – A. The representative hillslope profile obtained for W22 is shown as a pink overlay in Fig 3B. The catena length is chosen intuitively based on the relative elevation and distance from stream distribution plots (Fig 3B). The representative hillslope is then transferred to CATFLOW (Fig 3C) for simulating the catchment water balance.

For numerical simulation, the hillslope W22 was discretised into 531 (1 node for every 1 m) horizontal and 15 vertical elements. The total hillslope depth was set to 2 m, based on the transfer of knowledge from Weiherbach (see section 3.3). The vertical grid resolution varied from 0.05 m near the surface to 0.25 m towards the bottom node (Fig 3C). For ease of numerical simulation, we choose a uniform width (area of catchment/representative hillslope length) for all hillslope elements. Boundary conditions were set to the atmospheric boundary at the top and the no flow boundary at the left margin. Towards the lower boundary, a gravitational flow condition was established.

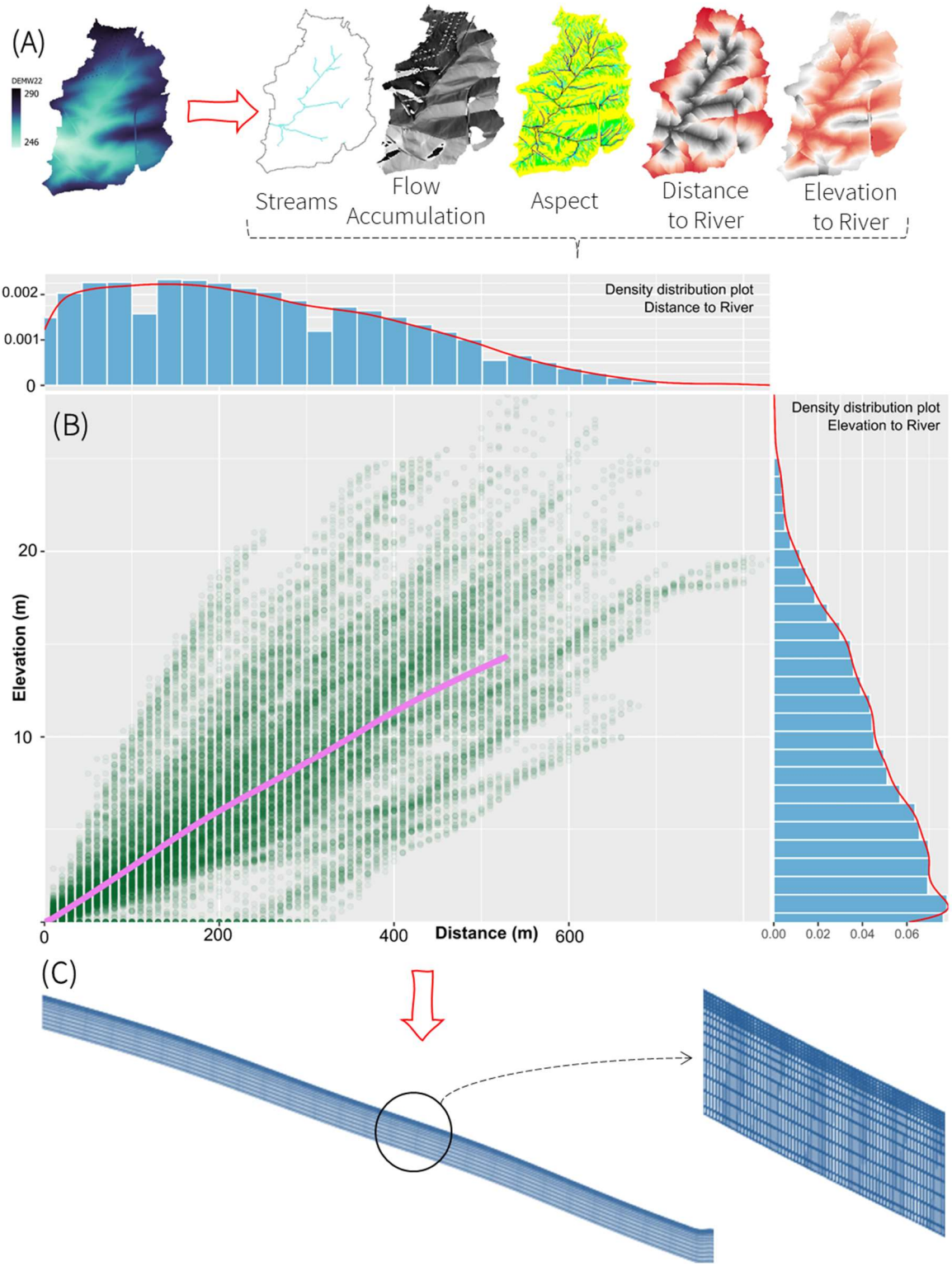

339 Figure 3 Workflow diagram illustrating the major steps involved in deriving the representative
340 hillslope catena for the catchment W22. Derivation of raster maps (streams, flow accumulation,
341 aspect, distance, elevation to river from the filled digital elevation model (DEM) (A). Selection and
342 binning of every distance and corresponding elevation to the nearest river segment (B).
343 Calculation of mean distance using flow accumulation weights (see also Appendix – A). Final
344 derived representative hillslope (pink overlay line in panel B) in panel C.

3.3 Transfer of System Parameters from Weiherbach

Since our present study area in the Elsenz-Schwarzbach consists mainly of agricultural loess catchments with similar geological and pedological characteristics of the previously monitored Weiherbach catchment (Zehe et al., 2001) and have the same major crops, we attempted a transfer of the soil and land use parameters from the previous field experiments (Fig 2-T).

A typical hillslope soil catena in the Weiherbach (Fig 2T: Zehe et al., 2001) consists of Calcaric Regosol (FAO/UNESCO, 1988; *Pararendzina*) or Luvisol (FAO/UNESCO, 1988; *Parabraunerde*) on top and mid slope sectors and Coluvisol (FAO/UNESCO, 1988; *Kolluvium*) in the hillslope foot. Hence, the representative hillslopes were assumed to have a similar distribution of soils along the downstream profile (Calcaric Regosol / Luvisol along 90% of the length of the hillslope and Coluvisol on the remaining 10%). The soil hydraulic functions based on the parameters of Mualem (1976) and van Genuchten (1980) were determined by Schäfer (1999) and Delbrück (1997) for the typical soils in the Weiherbach using both field and laboratory experiments (See Table 3 in Zehe et al. 2001). The same was utilized to set up the soil properties in the present study.

Estimates of surface roughness after the Manning-Strickler coefficient, K_{st}, for different crop types and maturity stages were obtained from more than 60 irrigation experiments conducted in the Weiherbach. (Throughout the remainder of this work, we use both Manning's roughness and Strickler values interchangeably to refer to the roughness coefficient (k) in the Gauckler-Manning-Strickler formula. Interested readers are referred to (Hager, 2015) for a historical anecdote). However, previous studies (Lumbroso and Gaume, 2012) have shown that the traditional estimates of the Manning's coefficient do not adequately represent flash flood conditions. Specifically, due to overbank flow during such extreme events, changes in the associated roughness properties are invariable. Hence, due to the high uncertainties involved in such calculations and the non-linear changes (e.g., overbank flow) typically seen during flash floods, we use an ensemble approach for the surface roughness. In principle, instead of running the model for one pre-selected Manning's roughness, we run the simulations for the range of Strickler values within the reported experiments in the Weiherbach (6-12 $m^{1/3}/s$) and report the mean and spread of the ensemble predictions.

As stated, CATFLOW also includes an advanced evapotranspiration subroutine, which enables time continuous simulations for a model spin up. However, use of this module requires detailed information about the relative fraction of each crop, which is not available for the summer of 2016, as well as detailed ground based data on radiation, wind speed, air humidity and temperature, which are neither at hand for our study area nor for most regions in the world. Hence, we decided not to use the inbuilt evapotranspiration module, but ran the model using globally available climate data sets for the model spin up. Specifically, we coupled the hillslope model with the climate reanalysis product ERA5 Land (Muñoz-Sabater et al., 2021), using precipitation and evapotranspiration during the event simulation and for model spin up as detailed in the next sections.

3.4 Initial and Boundary Conditions

The problem of inferring the initial conditions is a key challenge in all event-based modelling strategies (Beauchamp et al., 2013; Zeimetz et al., 2018). The challenge is usually not estimating the "actual" soil moisture state but establishing an initial state coherent with the land atmosphere interactions and parameterisations within the model (Koster et al., 2009). In essence, we seek an initialisation identical to the dynamics being captured by our model.

In the present work, we use the ERA5 Land hourly precipitation and evapotranspiration reanalysis data for initializing our representative hillslope model (Fig 2I) within a spin-up period of a year. The model was run using the mean catchment values of forcing data from ERA5 Land until the event of interest (8.06.2016 00:00 UTC); the corresponding soil moisture pattern was saved and then used as initial conditions for the event simulation with a radar based precipitation estimate (temporal resolution of 5 min) without recalibration.

During the event of 08 June 2016 (Appendix – B), there were no operational rainfall gauges that we know of, within the catchment area of Krebsbach. The nearest gauge operated by the Baden-Württemberg State Institute for the Environment, Survey and Nature Conservation (Landesanstalt für Umwelt, Messungen und Naturschutz Baden-Württemberg - LUBW) lay towards the southeast of catchment W22 in Bad Rappenau - Bonfeld (LUBW Station ID – 76730: Fig B1 in Appendix B). The gauge recorded a total precipitation sum of around 28 mm on 08 June. The German Weather Services (Deutscher

Wetterdienst -DWD) operates a nearby gauge in Waibstadt (DWD Station ID – 13674), west of catchment W44. The DWD gauge reported a total daily precipitation of 11 mm. Considering the mismatch between the two gauges and the need for a finer spatiotemporal estimate of the convective storm activity, we opt for a radar product (temporal resolution – 5 min) provided by Kachelmannwetter (Kachelmannwetter, n.d.) as the forcing boundary condition for the model. Appendix – B depicts radar images of the storm on 08.06.2016 over our study region. Overall, it can be seen that the storm activity is captured quite well by the fine resolution radar product. The direction of the storm also agrees with the smaller magnitude of total precipitation reported by the DWD gauge compared to the LUBW gauge (which seems to be nearer to the storm centre: Fig B1 in Appendix B).

4 Results

In the following section, we first showcase the initialisation using ERA5 Land and evaluate the performance of the hillslope models in describing the soil moisture changes at the annual scale (4.1). We then detail the event based flash flood simulations using the same representative hillslope models and radar based precipitation forcing in 4.2. Finally (4.3), we discuss the shape and LULC of the four catchments, and shed light on the potential to include spatially variable precipitation forcings for flash flood simulation using the representative hillslope approach.

4.1 Model Initialisation with ERA5 Land

Figure 4 shows the top soil (0-5 cm) water content simulated with the representative hillslope that was forced by ERA5 Land precipitation and evapotranspiration for catchment W22. Variations of Manning Strickler, K_{st} ($m^{1/3}/s$) leads to a variation in soil water content during the summer period. To characterize the coherence of these soil moisture simulation with the gridded ERA5 reanalysis product, we calculated the Kling-Gupta Efficiency (KGE) (Gupta et al., 2009) between the CATFLOW top layer soil moisture ensemble predictions with the spatially averaged ERA5 Land surface soil moisture (0-7 cm) (Fig 4 and Table 1).

While this revealed high KGE values, CATFLOW simulations were consistently drier than the ERA5 Land reanalysis product and the yearly CATFLOW runs (Figure 4). This mismatch likely reflects the different soil parameterizations and scale disparities in the two models. It is important to note that we do not expect perfect fit between the two

modeled soil moisture products, our interest is in capturing the overall local dynamics in soil moisture changes for such ungauged regions.

To better understand the relative role of such a bias in the overall KGE calculations, we also calculated the three components of the modified KGE (Pearson correlation, r and bias ratio, beta and variability ratio, gamma in Table 1) as per (Kling et al., 2012). As expected, we obtained high pearson correlation values (around 0.80) for all the different runs (varying Kst values). The high correlation shows that our approach reproduces the yearly dynamics of soil moisture changes in the region (using the coarse resolution globally available ERA5 Land data as a benchmark). The values of beta and gamma indicate the overall bias and variability of the modeled values compared to the ERA5 Land data.

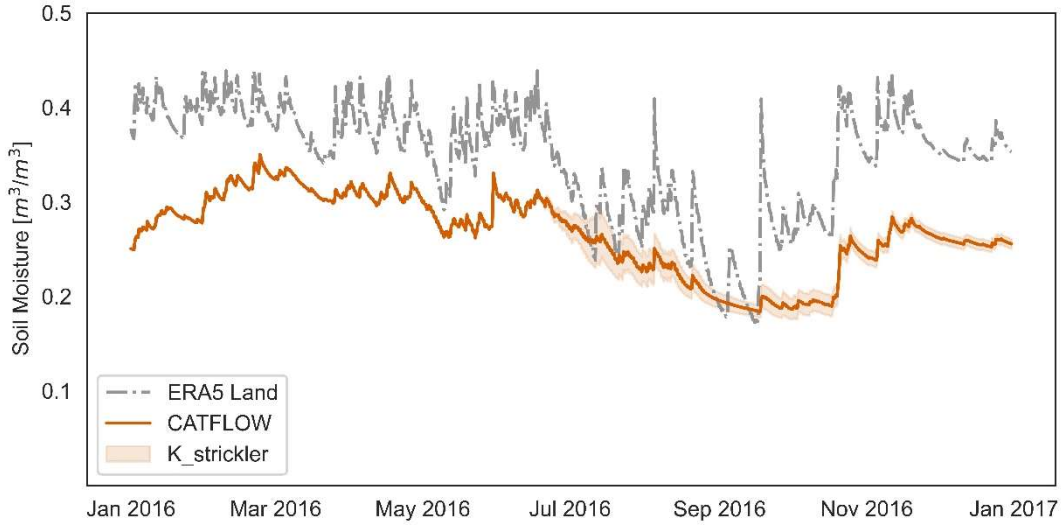

Figure 4: Time series of ERA5 Land surface soil moisture (0-7 cm) averaged over the entire catchment (grey) and the soil moisture simulations with CATFLOW (0-5 cm), red represents the ensemble mean, shaded regions depict the uncertainties (± the standard deviation) corresponding to different values of the Strickler coefficient (Kst = 6-12).

Table 1 Goodness of fit measures between the modeled soil moisture values of different CATFLOW runs (varying Manning Strickler coefficient K_{st}) with ERA5 Land surface soil moisture for catchment W22.

K_{st} ($m^{1/3}/s$)	**KGE**	**r**	**Gamma**	**Beta**
6	0.651	0.798	0.812	0.786
7	0.654	0.797	0.821	0.784
8	0.662	0.800	0.836	0.782
9	0.691	0.822	1.050	0.752

10	0.690	0.822	1.051	0.751
11	0.671	0.800	0.861	0.779
12	0.699	0.824	1.019	0.756

As we used ERA5 Land forcing variables (precipitation and evapotranspiration) to run the CATFLOW model, and then again ERA5 Land soil moisture states to evaluate the model performance, it remains to be seen whether the correlation is not only due to inherent, modeled dependencies within the reanalysis product. To shed light on this question, we again compared the CAFLOW simulations to another estimate of soil moisture for the same region, the in situ Soil Moisture Active Passive (Derksen et al., 2017) remote sensing product and obtained a decent (albeit lower) correlation value of r=0.61.

4.2 Flash flood modeling using representative hillslopes.

The representative hillslope models were then used to simulate the runoff response for the convective storm event on 08.06.2016 in the four catchments in the study area using the dynamical initial conditions obtained from the yearly scale runs using ERA5 Land. It is worth mentioning here that our approach of initializing the models using the reanalysis datasets helps in avoiding a random guess of the initial states and in complimenting parsimony principles. The approach also has implications for operationalization of the model (by changing the reanalysis product to a suitable nowcast product). Figure 5 displays the simulated catchment response modelled using a uniform precipitation series - the spatially averaged radar precipitation over each catchment (Appendix - B). The model performance in the four catchments is evaluated against the reconstructed inflow hydrograph obtained from the reservoir mass balance (Appendix – C) assuming relative measurement error measures for peak flow, volume, and time to peak as given in Table 2.

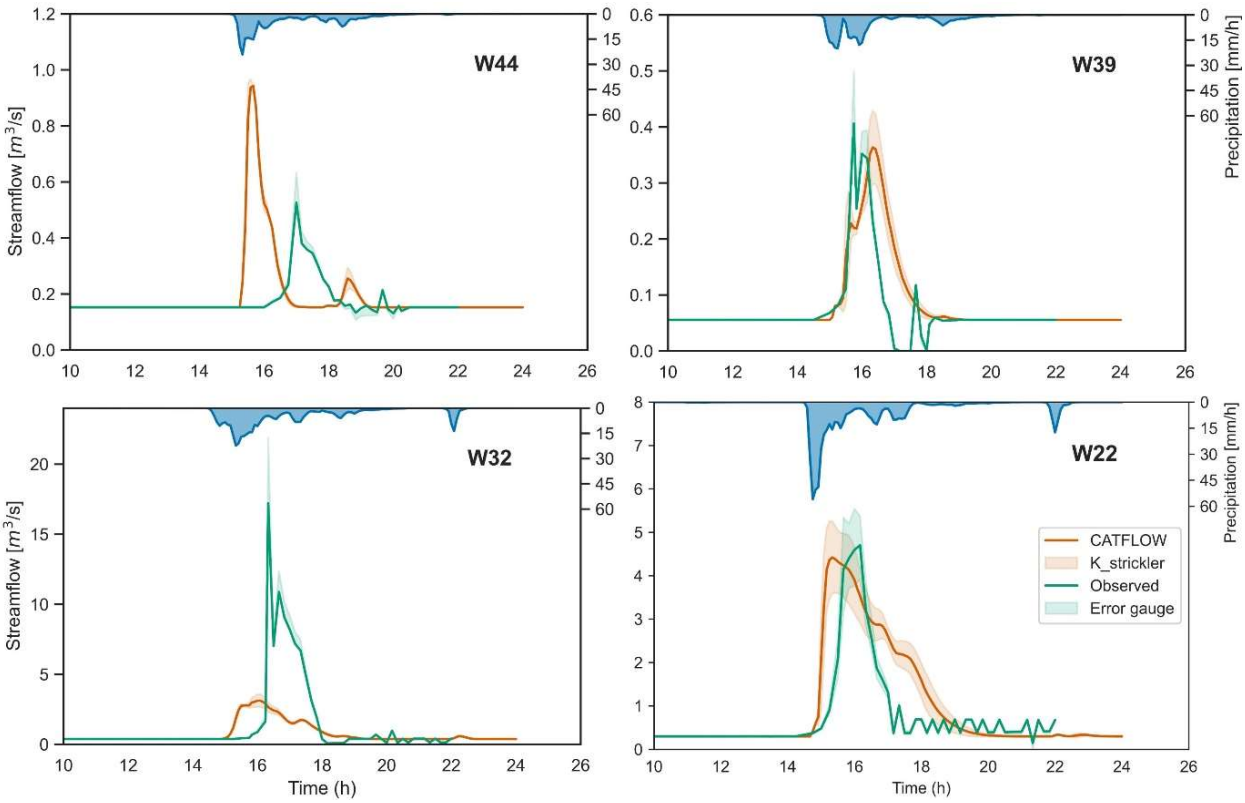

479 Figure 5: Rainfall – Runoff hydrographs for the flash flood event on 08.06.2016 at the four
480 headwater catchments (W22, W32, W39 and W44). Green curve indicates the reconstructed
481 inflow to the flood defence reservoir (Appendix – C), assuming measurement uncertainties of 5%.
482 Red curve indicates the mean values (± SD) of the predicted flood discharge by the CATFLOW
483 model ensemble (varying Strickler coefficient values). All simulation times are in UTC time zone.

484 Table 2: Characteristics of simulated and reconstructed storm hydrographs. The error values are
485 calculated between the mean values of the ensemble CATFLOW predictions and the inverted
486 flood hydrograph for each catchment. Area of each catchment is indicated in brackets.

Flood Characteristics	**W22 (2.91 km²)**		**W32 (5.6 km²)**		**W39 (0.73 km²)**		**W44 (2.44 km²)**	
	Obs	Sim	Obs	Sim	Obs	Sim	Obs	Sim
Storm Precipitation (mm)	49	-	35	-	26	-	24	-
Peak Discharge, Q (m^3/s)	4.703	4.421	17.212	3.123	0.406	0.363	0.527	0.943
Time of Peak, t (s)	58200	55200	58800	57900	56700	58800	61200	56400
Flood Volume, V (m^3)	45637	57978	72209	49868	5189	5959	13466	14537
Flood Volume, V (mm)	15.7	19.9	12.9	8.9	7.1	8.2	5.5	5.9
Runoff Coefficient, R	0.32	0.41	0.37	0.25	0.27	0.31	0.23	0.25

Percentage Error in Peak Discharge, P_Q(%)	-	6	-	82	-	11	-	-79
Error in time to Peak, P_t (s)	-	3000	-	900	-	-2100	-	4800
Percentage Error in Flood Volume, P_V (%)	-	-27	-	31	-	-15	-	-8

The model captures the steep ascent of the rising limb of the flood hydrograph, albeit with a time lag, and matches the magnitude of peak discharge values in at least two out of the four catchments (W22 and W39). Visually, the uncertainties in the simulated response due to changes in surface roughness are almost identical to the possible observational errors in the gauge level measurements (5%) that propagated into the estimated storm hydrograph.

More specifically, the peak flow errors (Table 1) in W22 (6%) and W39 (11%) are within the expected ranges considering the high uncertainties involved in local flash flood predictions. It is also interesting to note that the hillslope approach underestimates the peak flow magnitude but overestimates the flow volume for both the catchments. Also, the peak flow is delayed in W39 (happens later than observed) while it occurs earlier in W22.

On the contrary, in catchment W32, the hillslope model severely underestimates the storm response, while in W44 it slightly over predicts the discharge values. To better understand the apparent deviation in performance for catchments W32 and W44 compared to W22 and W39, we closely examined the storm pattern and then the relative shape, LULC and orientation of the catchments w.r.t the storm activity.

4.3 Role of LULC and distributed rainfall forcing

From Fig 1, we can observe that the catchments W32 and W44 appear to be more elongated and fan-shaped in contrast to the broader shaped catchments W22 and W39. Additionally, based on Fig 2P and details provided in Appendix B, the storm's direction suggests that our initial assumption of uniform precipitation across the representative hillslopes might not apply as neatly to the elongated catchments (W32 & W44).

However, the quite sharp discharge response of W32 (around 15 m^3/s within 15 minutes) seems unreasonably high when compared with the overall precipitation input and response in other catchments. One possible explanation could be an obstruction in the flow path perhaps due to debris like wood or sediment from the agricultural upstream areas of W32, which, as indicated by Fig B1 in Appendix B, was closer to the storm center.

This might have inadvertently created a temporary retention area, which then burst after a certain point, mimicking the effects of a dam break and resulting in a sudden inflow to the reservoir. Magnitude amplification due to such debris flows and driftwood blockages during flash floods have been reported in regions around the world (Chen et al., 2021; Schalko et al., 2018; Spreitzer et al., 2019).

The total event runoff coefficients calculated for each catchment (Table 2) also shows that while the approach slightly overestimates the response in all the other three catchments (W22, W39 and W44), it underrepresents the runoff response by around 12% in Catchment W32. One possible reason for the apparent stronger runoff production, might be the presence of larger fraction of impervious sealed built-up surface in W32. From Figure 1, it is seen that the small town of Haselbach lies within the catchment area, this contrasts to the other three catchments which are mostly only of agricultural or forest type (which also imposes limitations on the parameter transfer from the agricultural rural Weiherbach catchment). Another interesting point is that there is a well defined distribution of agricultural and forested areas along the stream profile in W32 (crops at the upstream plateaus and forest along the tributaries or near the outlet). These regions could hence behave like sub catchments having distinct concentration times.

However, it is worthwhile to note that out of all the four catchments the timing of the peak is most accurately captured in W32, which also has relevant implications for flood warning systems.

To investigate whether a distributed forcing input could help in better characterization of response in such elongated catchments, we again ran the simulations for catchments W32 and W44 using different rainfall time series along the representative hillslopes. Intuitively, we divided the catchment as having two different precipitation forcings over the upstream and downstream regions, to better reflect the storm pattern over the region (Appendix-B). Since this didn't lead to major changes for catchment W32 (apart from a minor increase in the peak flood), we only show the results for W44 in Fig 6. The predicted discharge values for catchment W44 are now remarkably close to the observed ones, relative peak errors reduce from around 80% to just 2% (Table 3). The relative volume error decreases to 2% from the earlier 8%, while the time to peak error remains nearly constant. This might be due to the longer stream network and the inability of the

hillslope approach to mimic the stream routing in such elongated hillslopes with more stream structures.

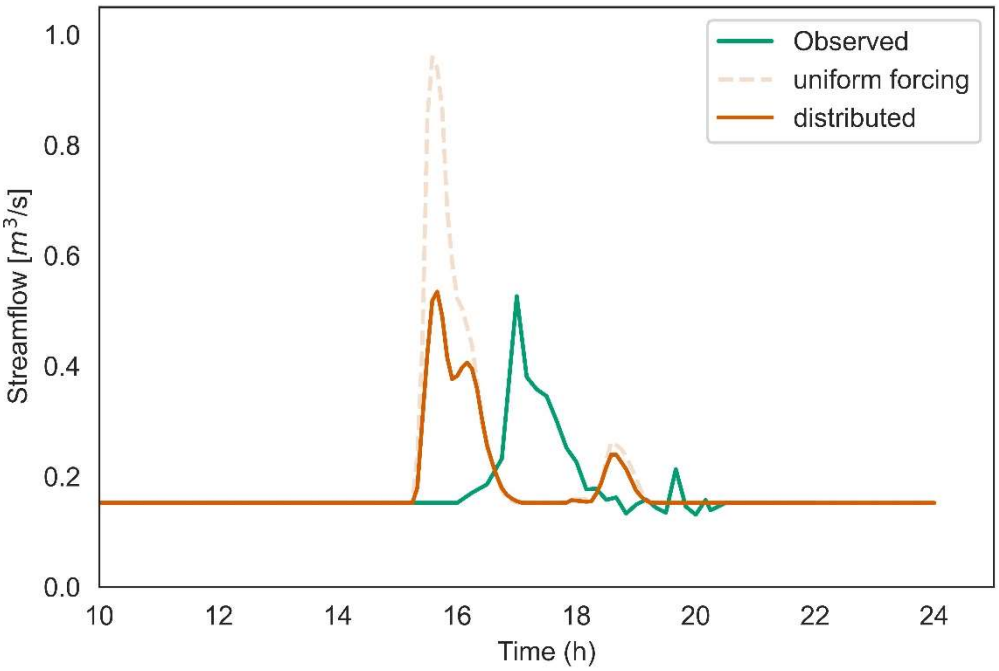

Figure 6 Flood hydrographs for catchment W44. Green curve indicates the reconstructed reservoir inflow, dotted red curve stands for model run using uniform precipitation forcing for the entire representative hillslope, solid red line denotes the model run with distributed forcing. All simulation times are in UTC time zone.

Table 3: Goodness of fit measures for the representative hillslope modelled discharges (K_{st} =9) with the reservoir stage inverted streamflow measures for distributed forcings over catchment W44.

Flood Characteristics	**W44 (2.44 km²)**		
	Observed	**Uniform forcing**	**Distributed forcing**
Peak Discharge, Q (m^3/s)	0.527	0.959	0.535
Time of Peak, t (s)	64800	56100	56400
Flood Volume, V (m^3)	13465.92	14567.44	13714.541
Runoff Coefficient, R	0.23	0.25	0.25
Percentage Error in Peak Discharge, P_Q (%)	-	-82.19	-1.52
Error in time to Peak, P_t (s)	-	53.13	50
Percentage Error in Flood Volume, P_V (%)	-	-8.18	-1.8

5 Discussion

In this study, we aimed to predict flash flood responses in data-scarce, small (<6 km^2) headwater catchments subjected to convective storm events. We utilized the representative hillslope concept and transferred parameters from a previous experimental catchment to establish process-based models for the four catchments under consideration. Given the absence of a comprehensive observational network in the area, we dynamically initialized initial conditions using climate reanalysis data. Furthermore, compared our event based simulations with reservoir streamflow inverted hydrographs. This comparison allowed us to quantify the relative simulation error values. Our endeavor to model and understand flood dynamics in these specific regions, despite the data limitations, gave crucial insights which presents a step forward in mitigation and preparation for such extreme events.

5.1 Towards short term predictability in ungauged basins

The Predictions in Ungauged Basin Initiative (IAHS PUB Initiative: Hrachowitz et al., 2013) attempted to bridge the gap in hydrologic predictions over ungauged basins by the concept of regionalization i.e to undertake a transfer of hydrological understanding from gauged to ungauged environments. Spatial proximity is one of the most widely used and simple regionalization techniques. The successful transfer of the previously obtained soil hydraulic parameters and the catena from the Weiherbach to the four Elsenz-Schwarzbach catchments, suggests that both could be valid in the entire hydrological landscape, the Kraichgau. The same applies to the crop specific Manning-Stricker parameters. In consequence, hydrological observatories like the Weiherbach (Zehe et al., 2001), the HOAL (Blöschl et al., 2016) or the Attert experimental basin (Pfister et al., 2017) could serve as donors for soil and vegetation parameters and behavioral hillslope setups within the same hydrological landscape.

Flash floods usually come as (bad) surprises, often impacting regions when and where we least expect them (Borga et al., 2008). Hence, strategies that provide robust warnings are essential. However, since they are also quite rare in nature, there lacks a coherent motivational starting point to invest time and resources into them (Montz and Gruntfest, 2002). In this study, we derived representative hillslope catenas for four head water catchments preserving their geopotential energy differences along the mean distance to the stream. Since, these representative catenas are thermodynamically consistent (based

on relative elevation differences and flow accumulation weighted mean values as discussed in Section 3.1 & Appendix -A) to the flow profiles in the catchment, we postulated that the representative hillslope should be able to provide reasonable estimates for rainfall-runoff prediction without the need for any manual event calibration.

While our approach provided near uncalibrated predictions for surface runoff in two out of the four catchments (W22 &W39), in the third catchment (W44), we had to release the assumption of uniform precipitation forcing over the hillslope and go for a distributed approach. The method was not able to capture the abrupt response in Catchment W32. However, as discussed in the text, the different landuse patterns within such elongated catchments implies that we may have to go for an approach involving different hillslopes for the different LULC classes and then add a suitable flow routing component to avoid the mismatch. In case they are not at hand, the soil hydraulic parameters (transferred from the experimental Weiherbach catchment in the current study: Table 3 in Zehe et al 2001) can be estimated using soil maps and textural data based on pedo-transfer functions (Rosetta: Schaap, 1999) for catchments of interest. The ensemble approach of using a range of roughness values helps overcome uncertainties involved in such parameters during extreme event simulations. This could be a first step in operationalization of such a flash flood event modeling system for small to lower mesoscale catchments with data gaps and scarcity issues.

5.2 Tackling data scarcity

Continuous simulations, for estimating initial conditions for the event simulations, were conducted using globally available climate reanalysis products (ERA5 Land). The importance of such antecedent soil moisture conditions in constraining the flood response cannot be overemphasized (Manoj J et al., 2023, 2022;), as has been shown for many catchments across Europe (Berghuijs et al., 2019; Blöschl et al., 2019, 2017). Global climate models have delivered commendable outcomes when it comes to capturing climate and weather extremes on regional scales. However, their potential in estimating the impacts of smaller scale hydrological events remains largely unexplored (IPCC, 2021; Poschlod, 2022). The representative hillslope approach which marries the beneficial components of lumped conceptual models with hydrological process based paradigms

could be a way forward to implement the vast knowledge of climate model simulations to smaller event scales.

Marchi et al. (2010) analysed around 25 major flash floods over Europe and showed that proper observational records didn't exist for more than half of the investigated events. During such intense flash floods, direct current meter measurements are often not possible due to safety and technical considerations. Furthermore, these events usually occur in remote ungauged regions with limited accessibility (Borga et al., 2008). It is important to stress here that even in cases with flow measurement gauges, prediction of discharge values during such convective events usually involves lot of uncertainties due to faulty devices, dynamical riverbed changes and floating debris in the stream (Lumbroso and Gaume, 2012). As is common in such poorly gauged catchments (Bronstert et al., 2018), we didn't have a streamflow gauge to compare our model performance, and hence we made use of the reservoir geometry and downstream flood retention reservoirs to obtain a crude estimate of the storm characteristics. This strategy creates a win-win situation, because local water resource managers are natural end users of such a warning system, and we tremendously increase the sample of historical test cases and complement the small sample that is available from the few gauging stations that observe catchments < 10 km^2.

5.3 Implications for Design Considerations

Natural streamflow variability has been altered by both climate change and anthropogenic water resources management policies (Pérez Ciria et al., 2019) over the last decades. Hence, it becomes imperative to consider multiple hydrological scenarios and a broader range of climatic forcings for the design of reservoirs and other flood control measures.

The evaluation and design of such hydraulic structures are generally based on univariate extreme values statistics, in Germany usually inferred from gridded KOSTRA rainfall extremes (Junghänel et al., 2017). These serve as input for event-based rainfall-runoff simulations using rather simple concepts such as the unit hydrograph hydrological models and in combinations with conceptual methods like the SCS-Curve number or rational method. This approach is essentially linear, which implies that the return period of the precipitation event determines the return period of flood runoff. Formation of flash

flood runoff is essentially non-linear, a 200-year precipitation event can cause a 10000 year flood, as observed for instance in the Weiherbach (Villinger et al., 2022).

Similarly, the flood reservoir W22 has been designed for a 100 year flood, though the precipitation event in 2016 had a return period (based on total precipitation) between 10 -20 years (Zehe et al, 2023) it still resulted in overflowing of the reservoir. In a different study we tested whether the event in 2016 could be reproduced using the simple FGM model (Ihringer, 1994 : the model uses the Unit Hydrograph method), that was used for designing the flood retention reservoir W22. This worked – but only after doubling the precipitation amount, which changes the return period from 20y to 200 - 500y. Thus underpinning, that standard estimators for runoff coefficients have deficiencies to cope with Hortonian overland flow and its strong dependence on precipitation intensity. This has crucial implications for the design and management of water resource infrastructure in a warming climate. Spatially distributed, process-based approaches that conserve both mass and momentum principles can incorporate multiple processes and complex feedbacks during the event. Ultimately, this helps to account for non-linear system responses and tipping points (L.Pimm, 1985).

Throughout Europe, record breaking summer heatwaves and droughts have been reported in recent years (Tripathy and Mishra, 2023: 2022 Compound Drought and Heat Wave). The occurrence of convective storm driven floods during summers have compounding effect on reservoir water management policies as water resources planners and reservoir operators face the daunting task of balancing the need for agricultural and irrigation water demand with the challenge of tackling flood risk. Efficient modeling and forecasting of flash floods could help mitigate the risk of such interconnected hazard cascades. Vegetative plant barriers (Richet et al., 2017) and other ecosystem based flood defence solutions (Temmerman et al., 2013) have also come up as a more sustainable and environmental friendly alternative to conventional manmade flood defense measures. The hillslope scale again emerges as an interesting sub-unit within a catchment (*virtual laboratories*: Fatichi et al., 2016) for testing the impact of such bio geomorphological measures on runoff response and sediment yield.

5.4 Limitations and Outlook

The perils of applying continuum-based models at scales for which the governing equations were not developed is well reviewed in literature (Hrachowitz and Clark,

2017). Such distributed, process-based approaches are also criticized for their complexity and larger data requirement compared to simple conceptual models. Conceptual (scaled-down) approaches on the other hand do not perform well in regions and scenarios which deviates from their well calibrated range of conditions (Fatichi et al., 2016; Hrachowitz and Clark, 2017). Hence, on balance, we believe that, under the threat of a non-stationary climate (Milly et al., 2008) and unprecedented flow regime changes, strategies which involve a convergence of different modelling philosophies are called for.

The representative hillslope approach for flash flood modelling is a venture in this regard. However, limitations remain that need to be properly understood and accounted for. The 2D effective representative hillslope used to represent the catchments implies the assumption of symmetry where the runoff production is controlled by hillslope parallel and vertical fluxes and their driving gradients (Loritz et al., 2017). The derived effective catena profile depicts our best guess based on the available topographical data (DEM). Any uncertainties and errors in the terrain representation will invariably propagate to our model geometry. Another point is the sensitivity to different DEM resolutions, raster filling and flow direction algorithms (Loritz et al., 2019).

So far, the flood simulations were essentially event based with no separate baseflow component (a constant baseflow was considered from start till end). Moreover, in our case, we do not attempt to fit the model response to the discharge curve obtained from the reservoir level measurements. Our main aim is to mimic the catchment response during such high intensity events in a simple, parsimonious manner. We also endeavored to consider the uncertainties in our modelled response (by varying the surface roughness) and the observational benchmark (relative error in gauge measurements). It is indeed true that the choice of process based model implies that we deal with a much larger number of system parameters and boundary conditions, compared to conceptual models. The strength is that these parameters are observable and, as shown in this study, transferable.

The forcings and soil moisture simulated by any land surface model (ERA5 Land, in our case) is highly model-dependent and direct transfer of one model product to another can lead to inconsistencies due to deviations in formulations (Koster et al., 2009). Attempting such a switch of forcing from a coarse gridded reanalysis product (ERA5 Land) to a fine

resolution radar precipitation product would usually entail a re-engineering of the model and associated variables. However, we show here that a process based, spatially distributed model can capture the dynamics due to their mechanistic description of the flow system (conserving both the energy and mass balances). Moreover, as we show in Section 4.1, we are more interested in the temporal soil moisture variability rather than the absolute values predicted by the models. Hence, we expect very less model bias due to the choice of the reanalysis product.

One argument frequently put against the use of process-based models in flash flood modelling and forecast strategies is their higher computational times. In the current attempt, we reiterate that by employing a representative approach which spatially averages along the main driving gradient of flow, we can preserve the total flow potential of the catchment without significant computational effort (For reference, the spin-up phase for the entire year had run time of less than 10 minutes while the event simulation for each catchment took around 2 minutes, in a normal Windows PC with 32GB RAM only).

Conclusions

The method of modeling flash floods in data-scarce, small headwaters using representative hillslopes, supplemented by climate reanalysis products, appears to be a viable pathway for achieving dependable rainfall-runoff simulations during high intensity storm events. By ensuring that these representative hillslopes align with the principles of thermodynamic conservation, we strike a balance between the intricacies required by physically based models and the desired simplicity rooted in parsimony considerations. Integrating with global climate reanalysis products effectively addresses the persistent challenges of data availability, a crucial aspect when modeling extreme events in data-limited regions globally. The findings indicate that the modeled hydrograph aligns well with the observed flood curve, derived from reservoir gauge level measurements, in three of the four studied catchments. While the approach demonstrated limitations in one of the region's larger catchments, further exploration and research, as outlined in the subsequent text, could provide more insights into modeling elongated catchments, especially those with urban developments.

Appendix – A (Energy considerations in the derivation of the representative hillslope catena)

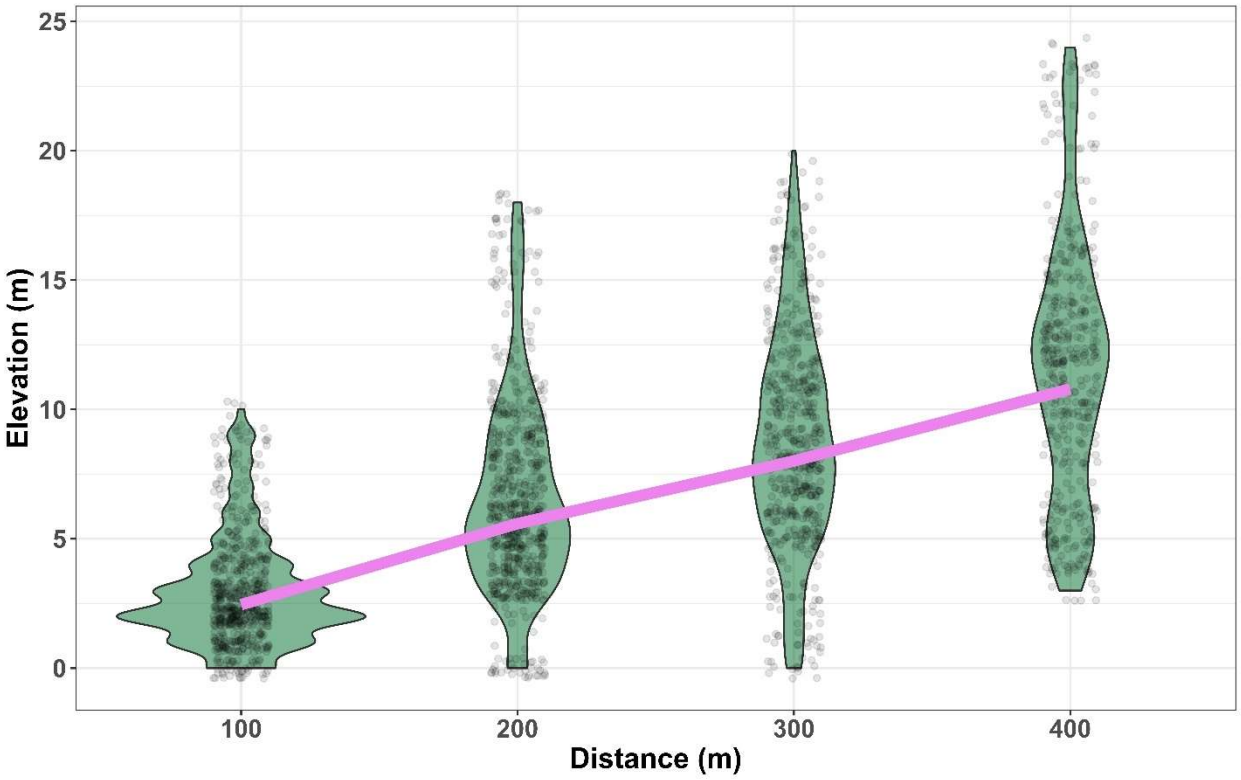

Figure A1 Plots showing the distribution of elevation values of each cell within four distinct distance classes from Fig 3B. The pink line denotes the representative hillslope profile derived from the mean elevation values using the approach detailed in Section 3.1.

From Newtonian mechanics, flow potential at a relative elevation (h) is defined as

$$E = m \times g \times h \tag{A1}$$

Where E is the potential energy of the water on the hillslope (J), m is its mass (kg), g represents the gravitational acceleration (m s^{-2}), and h is the relative height of the water above a reference (m).

For each class (say $x = l$ m), the average flow potential due to elevation values is related to the sum of the individual flow potential of all the cells (j: 1 to n) within the class

$$E_{avg}^{x=l} = \frac{E_{total}^{x=l}}{n} = \frac{\sum_{j=1}^{n} E_j^{x=l}}{n} \tag{A2}$$

754 The flow potential in the representative hillslope element at x = l m is given by:

$$\bar{E}^{x=l} = \bar{m} \times g \times \bar{h} \quad \text{(A3)}$$

755 Where $\bar{h}$ is the estimate of weighted mean elevation for a class at distance l ,calculated
756 using Eqn. 3.1 in Section 3.1. Table A1 shows these different energies for all the four
757 classes illustrated in Fig A1. On average, the relative errors between flow potential in the
758 classes and in the derived representative catena are seen to decrease as the distance from
759 the stream increases.

760 Table A1 The difference between the total flow potential in each class (Figure A1) and in the
761 derived representative hillslope in terms of density, ρ and gravitational acceleration, g.

Classes	$l = 100\ m$	$l = 200\ m$	$l = 300\ m$	$l = 400\ m$
$Energy\ in\ \ class\ , E_{avg}^{x=l}$	$301\rho g$	$660\rho g$	$877\rho g$	$1152\rho g$
$Energy\ in\ profile, \bar{E}^{x=l}$	$245\rho g$	$558\rho g$	$801\rho g$	$1079\rho g$
Relative Error (%)	-22.8	-18.28	-9.4	-6.7

Appendix – B (Storm Event on 08.06.2016)

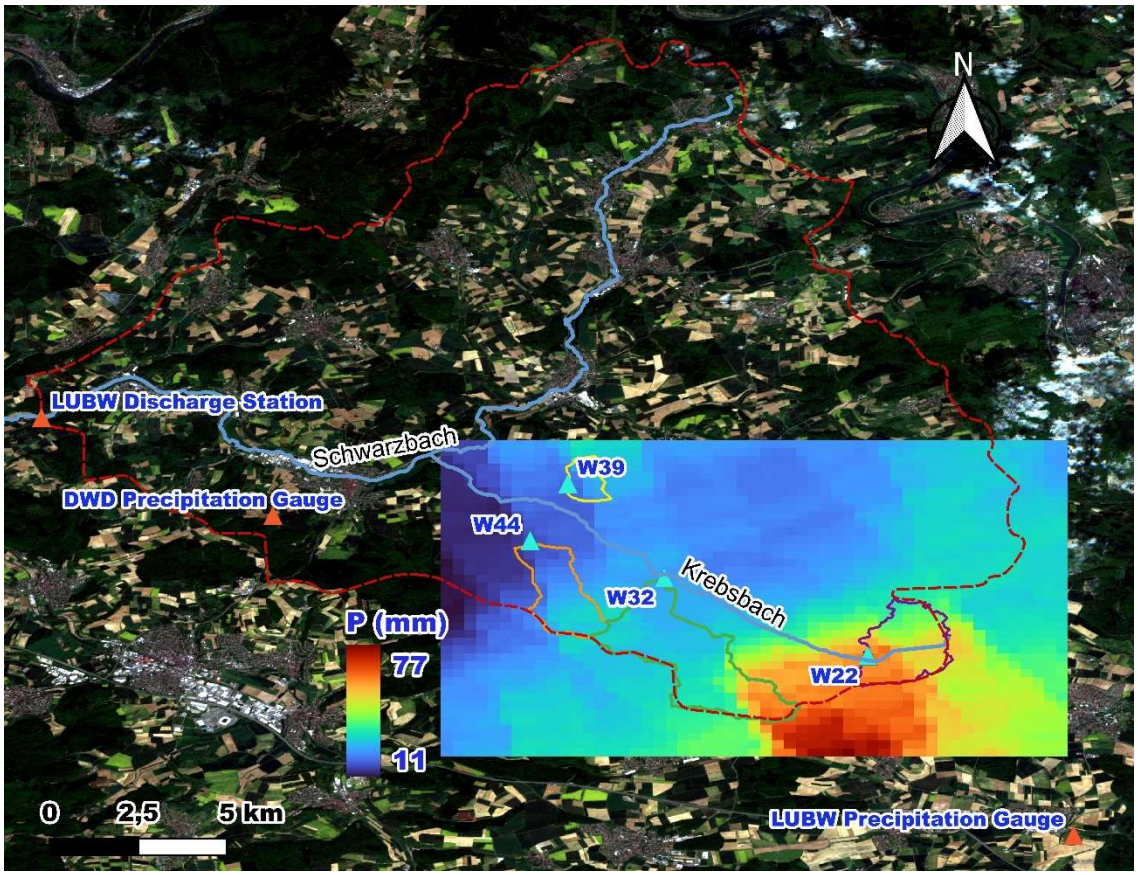

Figure B1 Overview of the Schwarzbach catchment till the LUBW streamflow station at Eschelbronn. In addition, the total accumulated precipitation (in mm) during the event is depicted as an overlay layer over the four catchments. Also, shown are the DWD and LUBW precipitation gauges.

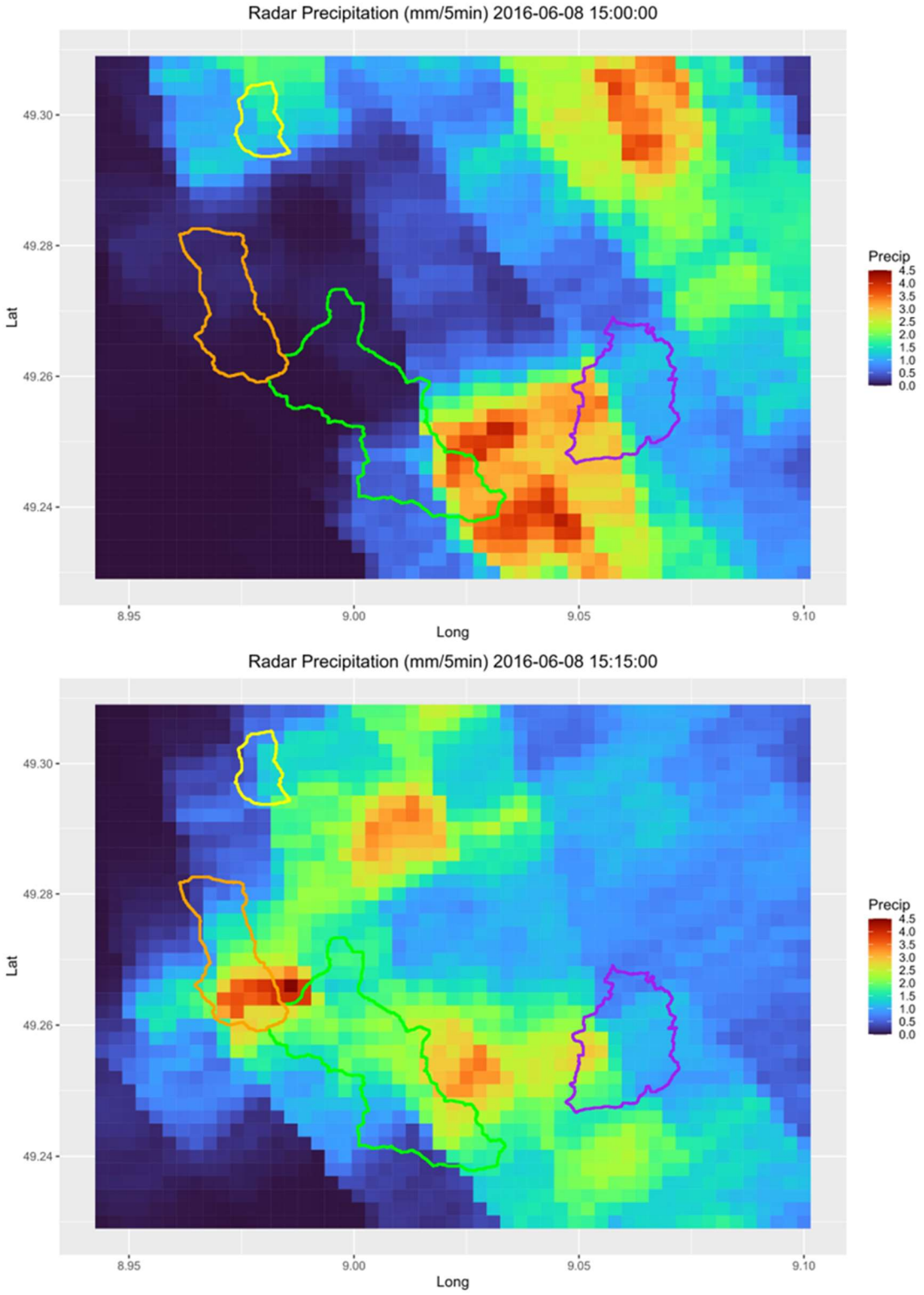

767 Figure B2 Evolution of the convective storm event on 08.06.2016 over the Krebsbach as captured
768 in the chosen radar based precipitation product (Kachelmannwetter, n.d.).

769 Figure B3 Impact of flash floods on 08.06.2016 over Catchment W22. (Zweckverband
770 Hochwasserschutz Elsenz-Schwarzbach)

Appendix – C (Flood estimation using reservoir mass balance)

Mass conservation has long been the foundation of hydrological modeling. This basic physical law is usually expressed (for hydrological systems) in the form of:

$$\frac{dS}{dt} = I(t) - O(t) \quad \text{(C1)}$$

where the change of a system's mass storage (S) with respect to time (t) is equal to total mass input, $I(t)$ minus total mass output, $O(t)$. This represents one of the most basic physical constraints placed on the functioning of any hydrological system.

Considering the mass balance of the downstream flood reservoirs in the four catchments (Fig 1 and B1) as shown in Fig C1, the storage in the reservoir at any time t being a function of the level (h). An automatic recorder measures the water level in the reservoir as shown in Fig C1. The outflow being again a function of the water level in the reservoir. Having knowledge of the reservoir geometry relations ($S = f(h)$) and the stage-discharge relationship of the outlet ($O = g(h)$), we now need to estimate the inflow to the reservoir from the catchment due to the convective storm activity. Again, from Eq C1:

$$\frac{dS}{dt} = I(t) - O(t) \quad \text{(C1)}$$

$$\frac{S(t + \Delta t, h + \Delta h) - S(t, h)}{\Delta t} = I(t) - O(t) \quad \text{(C2)}$$

Hence, the inflow is given by,

$$I(t) = \frac{S(t + \Delta t, h + \Delta h) - S(t, h)}{\Delta t} + O(t) \quad \text{(C3)}$$

Now for the uncertainty analysis, we consider a relative error of 5% in the reservoir level measurements and again calculate the inflows using Eq. C3. The inflow hydrograph obtained, and calculations are further shown for catchment W22 in Fig C2 and Table C1 respectively.

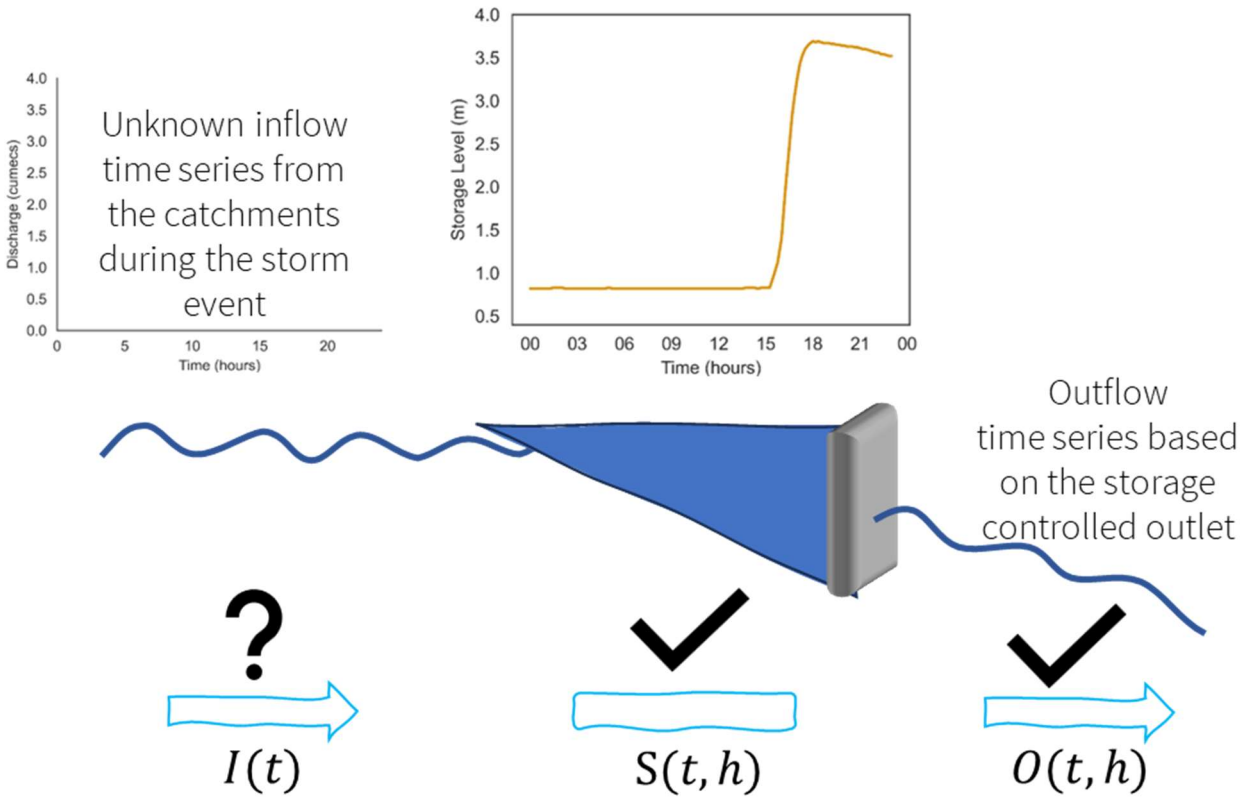

789 Figure C1 Schematic representation of the reservoir mass balance inversion

790 Table 2 Reservoir mass balance calculations for catchment W22

S No	Time	Level (m)	Storage (m^3)	Change in Storage (m^3)	Outflow (m^3/s)	Dt	Inflow (m^3/s)
63	08-06-2016 15:45	1.12	41.94883	16.42903	0.354373	900	0.372627
64	08-06-2016 16:00	1.4	107.4919	65.54307	0.407547	900	0.480373
65	08-06-2016 16:15	1.98	471.3575	363.8656	0.500051	900	0.904346
66	08-06-2016 16:30	2.48	1828.668	1357.311	0.565968	900	2.074091
67	08-06-2016 16:40	2.82	3952.833	2124.165	0.605154	600	4.145429
68	08-06-2016 16:50	3.06	6215.17	2262.337	0.631057	600	4.401619
69	08-06-2016 17:00	3.26	8583.66	2368.49	0.651033	600	4.598516
70	08-06-2016 17:10	3.43	11005.15	2421.491	0.666923	600	4.702742
71	08-06-2016 17:20	3.53	12547.01	1541.86	0.676144	600	3.245911
72	08-06-2016 17:30	3.6	13690.94	1143.932	0.68265	600	2.589203

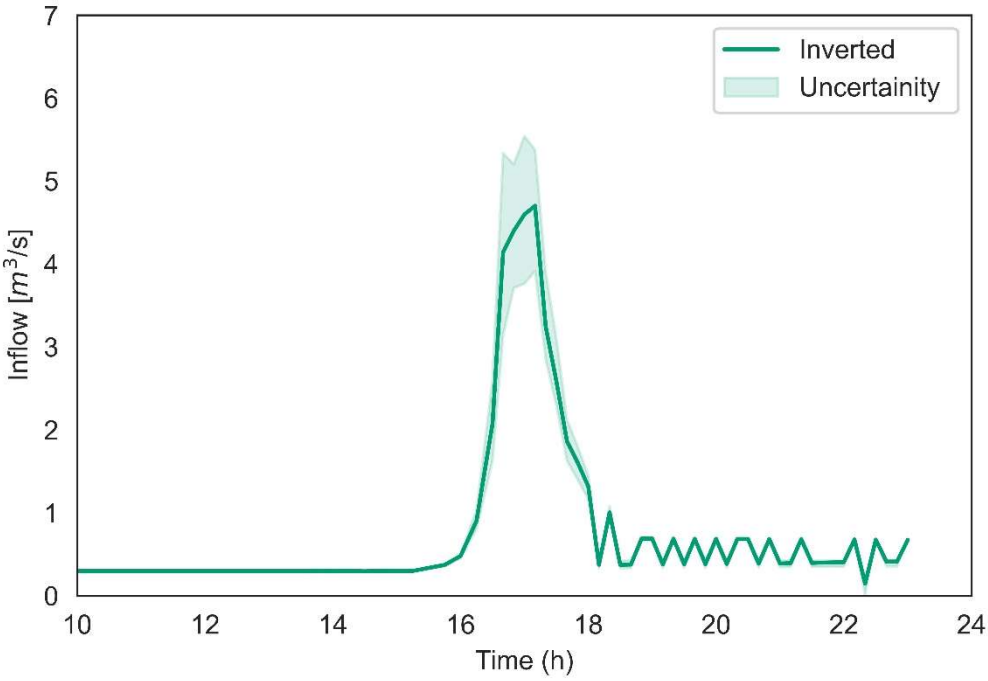

791 Figure C2 Reconstructed inflow time series for catchment W22. All times in CET.

Data Availability Statement

The ERA5 Land hourly data is freely available and can be accessed via the Copernicus Climate Change Services (C3S) Climate Data Store (https://cds.climate.copernicus.eu/cdsapp#!/dataset/reanalysis-era5-land?tab=overview). The simulation results can be found in Zenodo at (https://doi.org/10.5281/zenodo.8376684). All other data and codes used in this study are available on request from the corresponding author, Ashish Manoj J (ashish.jaseetha@kit.edu).

CRediT Author Contribution Statement

Ashish Manoj J: Data curation, Formal analysis, Investigation, Methodology, Conceptualization, Resources, Software, Validation, Visualization, Writing - original draft, review & editing. Ralf Loritz - Methodology, Resources, Validation, Supervision, Writing – review & editing. Franziska Villinger - Methodology, Conceptualization, Resources, Writing - review & editing. Mirko Mälicke – Software, Resources, Writing – review & editing. Mehdi Koopaeidar - Conceptualization, Writing – review & editing. Hans Göppert – Methodology, Conceptualization, Writing – review & editing. Erwin Zehe - Funding acquisition, Methodology, Conceptualization, Project administration, Supervision, Writing – review & editing.

Declaration of Competing Interest

The authors declare that they have no known competing financial interests or personal relationships that could have influenced the work reported in this paper.

Acknowledgements

This research contributes to the Implementation of an InfraStructure for dAta-BasEd Learning in environmental sciences (ISABEL) funded by the German Research Foundation (DFG). We would like to thank the Elsenz-Schwarzbach Water Board (Zweckverband Hochwasserschutz Elsenz-Schwarzbach) for providing the flood reservoir information and other relevant event data. We would also like to acknowledge all the stakeholders and original members of the Weiherbach project.

References

Beauchamp, J., Leconte, R., Trudel, M., Brissette, F., 2013. Estimation of the summer-fall PMP and PMF of a northern watershed under a changed climate. Water Resour. Res. 49, 3852–3862. https://doi.org/10.1002/wrcr.20336

Berghuijs, W.R., Harrigan, S., Molnar, P., Slater, L.J., Kirchner, J.W., 2019. The Relative Importance of Different Flood-Generating Mechanisms Across Europe. Water Resour. Res. 55, 2019WR024841. https://doi.org/10.1029/2019WR024841

Berkowitz, B., Zehe, E., 2020. Surface water and groundwater: unifying conceptualization and quantification of the two "water worlds." Hydrol. Earth Syst. Sci. 24, 1831–1858. https://doi.org/10.5194/hess-24-1831-2020

Beven, J.K., Binley, A., 1992. The future of distributed models: model calibration and uncertainty prediction. Hydrol. Process. 6, 265–277.

Blöschl, G., Blaschke, A.P., Broer, M., Bucher, C., Carr, G., Chen, X., Eder, A., Exner-Kittridge, M., Farnleitner, A., Flores-Orozco, A., Haas, P., Hogan, P., Kazemi Amiri, A., Oismüller, M., Parajka, J., Silasari, R., Stadler, P., Strauss, P., Vreugdenhil, M., Wagner, W., Zessner, M., 2016. The Hydrological Open Air Laboratory (HOAL) in Petzenkirchen: a hypothesis-driven observatory. Hydrol. Earth Syst. Sci. 20, 227–255. https://doi.org/10.5194/hess-20-227-2016

Blöschl, G., Hall, J., Parajka, J., Perdigão, R.A.P., Merz, B., Arheimer, B., Aronica, G.T., Bilibashi, A., Bonacci, O., Borga, M., Čanjevac, I., Castellarin, A., Chirico, G.B., Claps, P., Fiala, K., Frolova, N., Gorbachova, L., Gül, A., Hannaford, J., Harrigan, S., Kireeva, M., Kiss, A., Kjeldsen, T.R., Kohnová, S., Koskela, J.J., Ledvinka, O., Macdonald, N., Mavrova-Guirguinova, M., Mediero, L., Merz, R., Molnar, P., Montanari, A., Murphy, C., Osuch, M., Ovcharuk, V., Radevski, I., Rogger, M., Salinas, J.L., Sauquet, E., Šraj, M., Szolgay, J., Viglione, A., Volpi, E., Wilson, D., Zaimi, K., Živković, N., 2017. Changing climate shifts timing of European floods. Science (80-.). 357, 588–590. https://doi.org/10.1126/science.aan2506

Blöschl, G., Hall, J., Viglione, A., Perdigão, R.A.P., Parajka, J., Merz, B., Lun, D., Arheimer, B., Aronica, G.T., Bilibashi, A., Boháč, M., Bonacci, O., Borga, M., Čanjevac, I., Castellarin, A., Chirico, G.B., Claps, P., Frolova, N., Ganora, D., Gorbachova, L., Gül, A., Hannaford, J., Harrigan, S., Kireeva, M., Kiss, A., Kjeldsen, T.R., Kohnová, S., Koskela, J.J., Ledvinka, O., Macdonald, N., Mavrova-Guirguinova, M., Mediero, L., Merz, R., Molnar, P., Montanari, A., Murphy, C., Osuch, M., Ovcharuk, V., Radevski, I., Salinas, J.L., Sauquet, E., Šraj, M., Szolgay, J., Volpi, E., Wilson, D., Zaimi, K., Živković, N., 2019. Changing climate both increases and decreases European river floods. Nature 573, 108–111. https://doi.org/10.1038/s41586-019-1495-6

Blöschl, G., Kiss, A., Viglione, A., Barriendos, M., Böhm, O., Brázdil, R., Coeur, D., Demarée, G., Llasat, M.C., Macdonald, N., Retsö, D., Roald, L., Schmocker-Fackel, P., Amorim, I., Bělínová, M., Benito, G., Bertolin, C., Camuffo, D., Cornel, D., Doktor, R., Elleder, L., Enzi, S., Garcia, J.C., Glaser, R., Hall, J., Haslinger, K., Hofstätter, M., Komma, J., Limanówka, D., Lun, D., Panin, A., Parajka, J., Petrić, H., Rodrigo, F.S., Rohr, C., Schönbein, J., Schulte, L., Silva, L.P., Toonen, W.H.J., Valent, P., Waser, J., Wetter, O., 2020. Current European flood-rich period exceptional compared with past 500 years. Nature 583, 560–566. https://doi.org/10.1038/s41586-020-2478-3

Blöschl, G., Merz, R., Reszler, C., 2007. FLOODS IN AUSTRIA, in: Extreme Hydrological Events: New Concepts for Security. Springer Netherlands, Dordrecht, pp. 81–90. https://doi.org/10.1007/978-1-4020-5741-0_6

Borga, M., Anagnostou, E.N., Blöschl, G., Creutin, J.-D., 2011. Flash flood forecasting, warning and risk management: the HYDRATE project. Environ. Sci. Policy 14, 834–844. https://doi.org/10.1016/j.envsci.2011.05.017

Borga, M., Gaume, E., Creutin, J.D., Marchi, L., 2008. Surveying flash floods: gauging the ungauged extremes. Hydrol. Process. 22, 3883–3885. https://doi.org/10.1002/hyp.7111

Bremicker, M., 1998. Aufbau eines Wasserhaushaltsmodells für das Weser- und das Ostsee-Einzugsgebiet als Baustein eines Atmosphären-Hydrologie-Modells. PhD Thesis, Univ. Freibg.

Bronstert, A., Agarwal, A., Boessenkool, B., Crisologo, I., Fischer, M., Heistermann, M., Köhn-Reich, L., López-Tarazón, J.A., Moran, T., Ozturk, U., Reinhardt-Imjela, C., Wendi, D., 2018. Forensic hydro-meteorological analysis of an extreme flash flood: The 2016-05-29 event in Braunsbach, SW Germany. Sci. Total Environ. 630, 977–991. https://doi.org/10.1016/j.scitotenv.2018.02.241

Celia, M.A., Bouloutas, E.T., 1990. A general mass-conservative numerical solution for the unsaturated flow equation. . Water Resour. Res. 26, 483–1496.

Chen, J., Liu, W., Zhao, W., Jiang, T., Zhu, Z., Chen, X., 2021. Magnitude amplification of flash floods caused by large woody in Keze gully in Jiuzhaigou National Park, China. Geomatics, Nat. Hazards Risk 12, 2277–2299. https://doi.org/10.1080/19475705.2021.1961882

Delbrück, M., 1997. Großflächiges Bromidtracerexperiment zur räumlichen und zeitlichen Variabilität des Wassertransports an einem Lößhang. . Universität Heidelberg,, Dissertation.

Derksen, C., Xu, X., Scott Dunbar, R., Colliander, A., Kim, Y., Kimball, J.S., Black, T.A., Euskirchen, E., Langlois, A., Loranty, M.M., Marsh, P., Rautiainen, K., Roy, A., Royer, A., Stephens, J., 2017. Retrieving landscape freeze/thaw state from Soil Moisture Active Passive (SMAP) radar and radiometer measurements. Remote Sens. Environ. 194, 48–62. https://doi.org/10.1016/j.rse.2017.03.007

Drusch, M., Del Bello, U., Carlier, S., Colin, O., Fernandez, V., Gascon, F., Hoersch, B., Isola, C., Laberinti, P., Martimort, P., Meygret, A., Spoto, F., Sy, O., Marchese, F., Bargellini, P., 2012. Sentinel-2: ESA's Optical High-Resolution Mission for GMES Operational Services. Remote Sens. Environ. 120, 25–36. https://doi.org/10.1016/j.rse.2011.11.026

Dunne, T., Kirkby, M.J., 1978. Field studies of hillslope flow processes 227–293.

Fatichi, S., Vivoni, E.R., Ogden, F.L., Ivanov, V.Y., Mirus, B., Gochis, D., Downer, C.W., Camporese, M., Davison, J.H., Ebel, B., Jones, N., Kim, J., Mascaro, G., Niswonger, R., Restrepo, P., Rigon, R., Shen, C., Sulis, M., Tarboton, D., 2016. An overview of current applications, challenges, and future trends in distributed process-based models in hydrology. J. Hydrol. https://doi.org/10.1016/j.jhydrol.2016.03.026

906 Francke, T., Güntner, A., Mamede, G., Müller, E.N., Bronstert, A., 2008. Automated catena-
907 based discretization of landscapes for the derivation of hydrological modelling
908 units. Int. J. Geogr. Inf. Sci. 22, 111–132.
909 https://doi.org/10.1080/13658810701300873

910 Göppert, H., 2018. Auswertung von abgelaufenen Starkregenereignissen über
911 Radarmessungen. WASSERWIRTSCHAFT 108, 44–50.
912 https://doi.org/10.1007/s35147-018-0223-8

913 Gupta, H. V., Kling, H., Yilmaz, K.K., Martinez, G.F., 2009. Decomposition of the mean
914 squared error and NSE performance criteria: Implications for improving
915 hydrological modelling. J. Hydrol. 377, 80–91.
916 https://doi.org/10.1016/j.jhydrol.2009.08.003

917 Hager, W.H., 2015. Albert Strickler: His Life and Work. J. Hydraul. Eng. 141, 1–5.
918 https://doi.org/10.1061/(ASCE)HY.1943-7900.0001000

919 Horton, R.E., 1933. The role of infiltration in the hydrological cycle. Trans. Am. Geophys.
920 Union 14, 446–460.

921 Hrachowitz, M., Clark, M.P., 2017. HESS Opinions: The complementary merits of
922 competing modelling philosophies in hydrology. Hydrol. Earth Syst. Sci. 21, 3953–
923 3973. https://doi.org/10.5194/hess-21-3953-2017

924 Hrachowitz, M., Savenije, H.H.G., Blöschl, G., McDonnell, J.J., Sivapalan, M., Pomeroy, J.W.,
925 Arheimer, B., Blume, T., Clark, M.P., Ehret, U., Fenicia, F., Freer, J.E., Gelfan, A., Gupta,
926 H. V., Hughes, D.A., Hut, R.W., Montanari, A., Pande, S., Tetzlaff, D., Troch, P.A.,
927 Uhlenbrook, S., Wagener, T., Winsemius, H.C., Woods, R.A., Zehe, E., Cudennec, C.,
928 2013. A decade of Predictions in Ungauged Basins (PUB)-a review. Hydrol. Sci. J. 58,
929 1198–1255. https://doi.org/10.1080/02626667.2013.803183

930 Hundecha, Y., Bardossy, A., 2004. Modeling of the effect of land use changes on the
931 runoff generation of a river basin through parameter regionalization of a
932 watershed model. J. Hydrol. 292, 281–295.

933 Ihringer, J., 1994. Aufbau und Anwendung des Flußgebietsmodells “FGM.” DVWK
934 Fortbildungslehrgang Hydrol. "Niederschlag-Abfluß-Modelle Für Kleine
935 Einzugsgebiete Und Ihre Anwendung.

936 IPCC, 2021. Climate Change 2021: The Physical Science Basis. Contribution of Working
937 Group I to the Sixth Assessment Report of the Intergovernmental Panel on Climate
938 Change [Masson-Delmotte, V., P. Zhai, A. Pirani, S. L. Connors, C. Péan, S. Berger, N.
939 Caud, Y. Chen,. Cambridge Univ. Press 3949.

940 Jarvis, P.G., 1976. The Interpretation of the Variations in Leaf Water Potential and
941 Stomatal Conductance Found in Canopies in the Field Author (s): P . G . Jarvis
942 Source : Philosophical Transactions of the Royal Society of London . Series B ,
943 Biological Sciences , Publish. Philos. Trans. R. Soc. London 273, 593–610.

944 Junghänel, T., Ertel, H., Deutschländer, T., 2017. KOSTRA-DWD-2010R. Bericht zur
945 Revision der koordinierten Starkregenregionalisierung und-auswertung des
946 Deutschen Wetterdienstes in der Version 2010. KOSTRA-DWD-2010R - Bericht zur
947 Revis. der Koord. Starkregenregionalisierung und -auswertung des Dtsch.
948 Wetterdienstes der Version 2010.

949 Kachelmannwetter, n.d. Kachelmannwetter [WWW Document]. URL
950 https://kachelmannwetter.com/de

951 Klaus, J., Zehe, E., 2010. Modelling rapid flow response of a tile-drained field site using a
952 2D physically based model: assessment of "equifinal" model setups. Hydrol.
953 Process. 24, 1595–1609. https://doi.org/10.1002/hyp.7687

954 Kling, H., Fuchs, M., Paulin, M., 2012. Runoff conditions in the upper Danube basin under
955 an ensemble of climate change scenarios. J. Hydrol. 424–425, 264–277.
956 https://doi.org/10.1016/j.jhydrol.2012.01.011

957 Koster, R.D., Guo, Z., Yang, R., Dirmeyer, P.A., Mitchell, K., Puma, M.J., 2009. On the nature
958 of soil moisture in land surface models. J. Clim. 22, 4322–4335.
959 https://doi.org/10.1175/2009JCLI2832.1

960 L.Pimm, S., 1985. The complexity and stability of ecosystems. Nature 315, 635–636.

961 Loritz, R., Bassiouni, M., Hildebrandt, A., Hassler, S.K., Zehe, E., 2022. Leveraging sap flow
962 data in a catchment-scale hybrid model to improve soil moisture and transpiration
963 estimates. Hydrol. Earth Syst. Sci. 26, 4757–4771. https://doi.org/10.5194/hess-
964 26-4757-2022

965 Loritz, R., Hassler, S.K., Jackisch, C., Allroggen, N., van Schaik, L., Wienhöfer, J., Zehe, E.,
966 2017. Picturing and modeling catchments by representative hillslopes. Hydrol.
967 Earth Syst. Sci. 21, 1225–1249. https://doi.org/10.5194/hess-21-1225-2017

968 Loritz, R., Hrachowitz, M., Neuper, M., Zehe, E., 2021. The role and value of distributed
969 precipitation data in hydrological models. Hydrol. Earth Syst. Sci. 25, 147–167.
970 https://doi.org/10.5194/hess-25-147-2021

971 Loritz, R., Kleidon, A., Jackisch, C., Westhoff, M., Ehret, U., Gupta, H., Zehe, E., 2019. A
972 topographic index explaining hydrological similarity by accounting for the joint
973 controls of runoff formation. Hydrol. Earth Syst. Sci. 23, 3807–3821.
974 https://doi.org/10.5194/hess-23-3807-2019

975 Lumbroso, D., Gaume, E., 2012. Reducing the uncertainty in indirect estimates of
976 extreme flash flood discharges. J. Hydrol. 414–415, 16–30.
977 https://doi.org/10.1016/j.jhydrol.2011.08.048

978 Manoj J, A., Guntu, R.K., Agarwal, A., 2022. Spatiotemporal dependence of soil moisture
979 and precipitation over India. J. Hydrol. 610, 127898.
980 https://doi.org/10.1016/j.jhydrol.2022.127898

981 Manoj J, A., Pérez Ciria, T., Chiogna, G., Salzmann, N., Agarwal, A., 2023. Characterising
982 the coincidence of soil moisture – precipitation extremes as a possible precursor to
983 European floods. J. Hydrol. 620, 129445.
984 https://doi.org/10.1016/j.jhydrol.2023.129445

985 Marchi, L., Borga, M., Preciso, E., Gaume, E., 2010. Characterisation of selected extreme
986 flash floods in Europe and implications for flood risk management. J. Hydrol. 394,
987 118–133. https://doi.org/10.1016/j.jhydrol.2010.07.017

988 Marchi, L., Cavalli, M., Amponsah, W., Borga, M., Crema, S., 2016. Upper limits of flash
989 flood stream power in Europe. Geomorphology 272, 68–77.
990 https://doi.org/10.1016/j.geomorph.2015.11.005

991 Meyer, J., Neuper, M., Mathias, L., Zehe, E., Pfister, L., 2022. Atmospheric conditions
992 favouring extreme precipitation and flash floods in temperate regions of Europe.
993 Hydrol. Earth Syst. Sci. 26, 6163–6183. https://doi.org/10.5194/hess-26-6163-
994 2022

995 Milly, P.C.D., Betancourt, J., Falkenmark, M., Hirsch, R.M., Kundzewicz, Z.W., Lettenmaier,
996 D.P., Stouffer, R.J., 2008. Climate change: Stationarity is dead: Whither water
997 management? Science (80-.). 319, 573–574.
998 https://doi.org/10.1126/science.1151915

999 Montz, B.E., Gruntfest, E., 2002. Flash flood mitigation: Recommendations for research
1000 and applications. Environ. Hazards 4, 15–22.
1001 https://doi.org/10.3763/ehaz.2002.0402

1002 Mualem, Y., 1976. A new model for predicting the hydraulic conductivity of unsaturated
1003 porous media. Water Resour. Res. 12, 513–522.
1004 https://doi.org/10.1029/WR012i003p00513

1005 Munich Re, 2016. Munich Re [WWW Document]. URL
1006 https://www.munichre.com/en/company/media-relations/media-information-
1007 and-corporate-news/media-information/2016/2016-07-12-media-
1008 information.html

1009 Muñoz-Sabater, J., Dutra, E., Agustí-Panareda, A., Albergel, C., Arduini, G., Balsamo, G.,
1010 Boussetta, S., Choulga, M., Harrigan, S., Hersbach, H., Martens, B., Miralles, D.G.,
1011 Piles, M., Rodríguez-Fernández, N.J., Zsoter, E., Buontempo, C., Thépaut, J.-N., 2021.
1012 ERA5-Land: a state-of-the-art global reanalysis dataset for land applications. Earth
1013 Syst. Sci. Data 13, 4349–4383. https://doi.org/10.5194/essd-13-4349-2021

1014 Pall, P., Allen, M.R., Stone, D.A., 2007. Testing the Clausius–Clapeyron constraint on
1015 changes in extreme precipitation under CO2 warming. Clim. Dyn. 28, 351–363.
1016 https://doi.org/10.1007/s00382-006-0180-2

1017 Paniconi, C., Putti, M., 2015. Physically based modeling in catchment hydrology at 50:
1018 Survey and outlook. Water Resour. Res. 51, 7090–7129.
1019 https://doi.org/10.1002/2015WR017780

1020 Pérez, A.J., Abrahão, R., Causapé, J., Cirpka, O.A., Bürger, C.M., 2011. Simulating the
1021 transition of a semi-arid rainfed catchment towards irrigation agriculture. J. Hydrol.
1022 409, 663–681. https://doi.org/10.1016/j.jhydrol.2011.08.061

1023 Pérez Ciria, T., Labat, D., Chiogna, G., 2019. Detection and interpretation of recent and
1024 historical streamflow alterations caused by river damming and hydropower
1025 production in the Adige and Inn river basins using continuous, discrete and
1026 multiresolution wavelet analysis. J. Hydrol. 578, 124021.
1027 https://doi.org/10.1016/j.jhydrol.2019.124021

1028 Peters, A., Hohenbrink, T.L., Iden, S.C., Durner, W., 2021. A Simple Model to Predict
1029 Hydraulic Conductivity in Medium to Dry Soil From the Water Retention Curve.
1030 Water Resour. Res. 57. https://doi.org/10.1029/2020WR029211

1031 Pfister, L., Martinez-Carreras, N., Hissler, C., Klaus, J., Carrer, G.E., Stewart, M.K.,
1032 McDonnell, J.J., 2017. Bedrock geology controls on catchment storage, mixing, and
1033 release: A comparative analysis of 16 nested catchments. Hydrol. Process. 31,

1828–1845. https://doi.org/10.1002/hyp.11134

Piper, D., Kunz, M., Ehmele, F., Mohr, S., Mühr, B., Kron, A., Daniell, J., 2016. Exceptional sequence of severe thunderstorms and related flash floods in May and June 2016 in Germany - Part 1: Meteorological background. Nat. Hazards Earth Syst. Sci. 16, 2835–2850. https://doi.org/10.5194/nhess-16-2835-2016

Plate, E., Zehe, E., 2008. Hydrologie und Stoffdynamik kleiner Einzugsgebiete. Prozesse und Modelle. Schweizerbart'sche Verlagsbuchhandlung.

Poschlod, B., 2022. Attributing heavy rainfall event in Berchtesgadener Land to recent climate change – Further rainfall intensification projected for the future. Weather Clim. Extrem. 38, 100492. https://doi.org/10.1016/j.wace.2022.100492

Reggiani, P., Hassanizadeh, S.M., Sivapalan, M., 1998. A unifying framework for watershed thermodynamics: balance equations for mass, momentum, energy and entropy, and the second law of thermodynamics. Adv. Water Resour. 22, 367–398.

Remson, I., Hornberger, G.M., Molz, F.J., 1971. Numerical Methods in Subsurface Hydrology, With an Introduction to the Finite Element Method. Wiley-Interscience.

Richet, J.-B., Ouvry, J.-F., Saunier, M., 2017. The role of vegetative barriers such as fascines and dense shrub hedges in catchment management to reduce runoff and erosion effects: Experimental evidence of efficiency, and conditions of use. Ecol. Eng. 103, 455–469. https://doi.org/10.1016/j.ecoleng.2016.08.008

Ruiz-Villanueva, V., Borga, M., Zoccatelli, D., Marchi, L., Gaume, E., Ehret, U., 2012. Extreme flood response to short-duration convective rainfall in South-West Germany. Hydrol. Earth Syst. Sci. 16, 1543–1559. https://doi.org/10.5194/hess-16-1543-2012

Schaap, M.G., 1999. Rosetta.

Schäfer, D., 1999. Bodenhydraulischen Funktionen eines Kleineinzugsgebiets –Vergleich und Bewertung unterschiedlicher Verfahren. . Dissertation, Institute of Hydromechanics, University of Karlsruhe, Germany. .

Schalko, I., Schmocker, L., Weitbrecht, V., Boes, R.M., 2018. Backwater Rise due to Large Wood Accumulations. J. Hydraul. Eng. 144, 1–13. https://doi.org/10.1061/(asce)hy.1943-7900.0001501

Schroers, S., Eiff, O., Kleidon, A., Scherer, U., Wienhöfer, J., Zehe, E., 2022. Morphological controls on surface runoff: An interpretation of steady-state energy patterns, maximum power states and dissipation regimes within a thermodynamic framework. Hydrol. Earth Syst. Sci. 26, 3125–3150. https://doi.org/10.5194/hess-26-3125-2022

Schroers, S., Scherer, U., Zehe, E., 2023. Energy efficiency in transient surface runoff and sediment fluxes on hillslopes – a concept to quantify the effectiveness of extreme events. Hydrol. Earth Syst. Sci. 27, 2535–2557. https://doi.org/10.5194/hess-27-2535-2023

Sivapalan, M., Takeuchi, K., Franks, S.W., Gupta, V.K., Karambiri, H., Lakshmi, V., Liang, X., McDonnell, J.J., Mendiondo, E.M., O'Connell, P.E., Oki, T., Pomeroy, J.W., Schertzer, D., Uhlenbrook, S., Zehe, E., 2003. IAHS Decade on Predictions in Ungauged Basins

(PUB), 2003-2012: Shaping an exciting future for the hydrological sciences. Hydrol. Sci. J. 48, 857–880. https://doi.org/10.1623/hysj.48.6.857.51421

Spreitzer, G., Tunnicliffe, J., Friedrich, H., 2019. Using Structure from Motion photogrammetry to assess large wood (LW) accumulations in the field. Geomorphology 346, 106851. https://doi.org/10.1016/j.geomorph.2019.106851

Steinbrich, A., Leistert, H., Weiler, M., 2016. Model-based quantification of runoff generation processes at high spatial and temporal resolution. Environ. Earth Sci. 75, 1–16. https://doi.org/10.1007/s12665-016-6234-9

Tang, Y.K., Skaggs, R.W., 1977. Experimental evaluation of theoretical solutions for subsurface drainage and irrigation. Water Resour. Res. 13, 957–965. https://doi.org/10.1029/WR013i006p00957

Temmerman, S., Meire, P., Bouma, T.J., Herman, P.M.J., Ysebaert, T., De Vriend, H.J., 2013. Ecosystem-based coastal defence in the face of global change. Nature 504, 79–83. https://doi.org/10.1038/nature12859

Thielen, J., Bartholmes, J., Ramos, M.-H., de Roo, A., 2009. The European Flood Alert System – Part 1: Concept and development. Hydrol. Earth Syst. Sci. 13, 125–140. https://doi.org/10.5194/hess-13-125-2009

Tripathy, K.P., Mishra, A.K., 2023. How Unusual Is the 2022 European Compound Drought and Heatwave Event? Geophys. Res. Lett. 50. https://doi.org/10.1029/2023GL105453

Troch, P.A., Paniconi, C., Emiel van Loon, E., 2003. Hillslope-storage Boussinesq model for subsurface flow and variable source areas along complex hillslopes: 1. Formulation and characteristic response. Water Resour. Res. 39. https://doi.org/10.1029/2002WR001728

van der Knijff, J.M., Younis, J., de Roo, A.P.J., 2010. LISFLOOD: A GIS-based distributed model for river basin scale water balance and flood simulation. Int. J. Geogr. Inf. Sci. 24, 189–212. https://doi.org/10.1080/13658810802549154

van Genuchten, M.T., 1980. A Closed-form Equation for Predicting the Hydraulic Conductivity of Unsaturated Soils. Soil Sci. Soc. Am. J. 44, 892–898. https://doi.org/10.2136/sssaj1980.03615995004400050002x

Villinger, F., Loritz, R., Zehe, E., 2022. Physically based simulation of an occurred flash flood using “representative hillslopes” in a rural catchment. Hydrol. und Wasserbewirtschaftung 66, 286–297. https://doi.org/10.5675/HyWa_2022.6_1

Wienhofer, J., Zehe, E., 2014. Predicting subsurface stormflow response of a forested hillslope - the role of connected flow paths. Hydrol. Earth Syst. Sci. 18, 121–138. https://doi.org/10.5194/hess-18-121-2014

Zehe Villinger, F. Loritz, R. Koopaeidar,M. Göppert. H., E., 2023. Physikalisch basierte Simulation von Sturzfluten in kleinen ländlichen Gebieten – eine Option für die Bemessungspraxis. . Korrespondenz Wasserwirtschaft 16, 108–118. https://doi.org/https://doi.org/10.3243/kwe2023.02.004

Zehe, E., Becker, R., Bardossy, A., Plate, E., 2005. Uncertainty of simulated catchment runoff response in the presence of threshold processes: Role of initial soil moisture

and precipitation. J. Hydrol. 315, 183–202.

Zehe, E., Blöschl, G., 2004. Predictability of hydrologic response at the plot and catchment scales: Role of initial conditions. Water Resour. Res. 40. https://doi.org/10.1029/2003WR002869

Zehe, E., Ehret, U., Blume, T., Kleidon, A., Scherer, U., Westhoff, M., 2013. A thermodynamic approach to link self-organization, preferential flow and rainfall-runoff behaviour. Hydrol. Earth Syst. Sci. 17, 4297–4322. https://doi.org/10.5194/hess-17-4297-2013

Zehe, E., Ehret, U., Pfister, L., Blume, T., Schroder, B., Westhoff, M., Jackisch, C., Schymanski, S.J., Weiler, M., Schulz, K., Allroggen, N., Tronicke, J., van Schaik, L., Dietrich, P., Scherer, U., Eccard, J., Wulfmeyer, V., Kleidon, A., 2014. HESS Opinions: From response units to functional units: a thermodynamic reinterpretation of the HRU concept to link spatial organization and functioning of intermediate scale catchments. Hydrol. Earth Syst. Sci. 18, 4635–4655. https://doi.org/10.5194/hess-18-4635-2014

Zehe, E., Maurer, T., Ihringer, J., Plate, E., 2001. Modelling water flow and mass transport in a Loess catchment. Phys. Chem. Earth, Part B 26, 487–507. https://doi.org/10.1016/S0378-3774(99)00083-9

Zeimetz, F., Schaefli, B., Artigue, G., García Hernández, J., Schleiss, A.J., 2018. New Approach to Identifying Critical Initial Conditions for Extreme Flood Simulations in a Semicontinuous Simulation Framework. J. Hydrol. Eng. 23, 1–9. https://doi.org/10.1061/(asce)he.1943-5584.0001652

Zweckverband Hochwasserschutz Elsenz-Schwarzbach, 2016. Elsenz-Schwarzbach Water Board [WWW Document]. URL https://www.zvhws.de/